POLITECNICO
MILANO 1863

SCUOLA DI INGEGNERIA INDUSTRIALE
E DELL'INFORMAZIONE

Wake Modeling for Downstream Wind Turbine Fatigue Load Estimation

Tesi di Laurea Magistrale in
Energy Engineering - Ingegneria energetica

Author: **Andrea Rossi**

Student ID: 990326
Advisor: Prof. Alessandro Croce
Co-advisors: Stefano Cacciola
Academic Year: 2023-2024

Abstract

Due to reductions in installation and maintenance costs, wind turbines are often clustered in arrays, commonly referred to as wind farms. As the wind farms get denser, the generators spend increasingly more time in the wake of other turbines with negative repercussions on the power production and possibly on the loading of the machines. To reduce the effects of this phenomenon a shift in optimization perspective is necessary, from the single turbine to the overall wind farm. This is done by controlling the upstream turbines by either steering the wake away through a yaw angle misalignment or by reducing the energy extracted from the wind through axial induction factor reduction so that the downstream turbines experience a more energetic and stable inflow. While a previous work[1] has shown the potential of these strategies from a power production point of view, their effect on the fatigue loads of the downstream turbine is yet to be included. This thesis aims at bridging this gap by proposing a computationally light approach for evaluating fatigue loads on downstream wind turbines. To achieve this goal, firstly a very fast steady state open source code is employed to obtain the steady state wake properties of the wake generated by a state-of-the-art turbine for a range of different operational and environmental conditions. The inflow necessary for the aeroelastic software to calculate the loads history, is then obtained by dividing the wind into two regions, one with the properties of the steady state wake and added wake turbulence and another one where no wake effects are present. Through 220 aeroelastic simulations of 10 minutes each a look up table is then built and by interpolating over it the fatigue loads can be obtained for each condition in the initial domain. Results show that, for the cases considered, by operating in the wake the downstream turbine is always characterized by higher fatigue loads compared to the upstream generator. Nonetheless if compared to the uncontrolled condition, for the flapwise and fore-aft load some control combinations can reduce the DELs by respectively 8 % and 6 %.

Keywords: wind turbines, fatigue load, FLORIS, wake control, wind farm

Abstract in lingua italiana

A causa dei costi di installazione e manutenzione ridotti, le turbine eoliche sono spesso raggruppate in schiere, comunemente chiamate parchi eolici. Man mano che i parchi eolici diventano più fitti, i generatori spendono sempre più tempo nella scia di altre turbine con ripercussione negative sulla produzione di potenza e potenzialmente anche su i carichi delle macchine. Per ridurre gli effetti di questo fenomeno è necessario, durante l'ottimizzazione, spostare l'attenzione dalla singola turbina all'intero parco eolico. Ciò avviene controllando le turbine a monte, allontanando la scia attraverso un disallineamento dell'angolo di imbardata oppure riducendo l'energia estratta dal vento attraverso una riduzione del fattore di induzione assiale in modo che la turbina a valle senta un influsso più energico e stabile. Sebbene uno studio precedente [1] ha mostrato il potenziale di queste strategie dal punto di vista della produzione di potenza, il loro effetto sui carichi di fatica della turbina a valle non è ancora stato considerato. Questa tesi si propone di colmare questa lacuna proponendo un approccio computazionalmente leggero per valutare i carichi a fatica di turbine a valle. Per questo obiettivo, in primo luogo è stato utilizzato un codice open source molto veloce per ottenere le proprietà della scia generata da una turbina allo stato dell'arte in stato stazionario per una serie di diverse condizioni operative e ambientali. L'influsso necessario per il software aeroelastico per calcolare la storia dei carichi, viene ottenuta dividendo il vento in due regioni, una con le proprietà della scia in stato stazionario e con una turbolenza di scia aumentata e un'altra in cui non sono presenti effetti di scia. Attraverso 220 simulazioni aeroelastiche di 10 minuti ciascuna, viene costruita la tabella dati e, interpolando su di essa, si possono ottenere i carichi a fatica per ogni condizione del dominio iniziale. I risultati mostrano che, per i casi considerati, lavorando nella scia, la turbina a valle è sempre caratterizzata da carichi a fatica più elevati rispetto al generatore a monte. Tuttavia, se paragonata alla condizione non controllata, per il carico flapwise e fore-aft alcune combinazioni di controllo possono ridurre i DEL rispettivamente dell'8 % e del 6 %.

Parole chiave: turbine eoliche, carichi a fatica, FLORIS, controllo di scia, parco eolico

Contents

1 | Introduction

In recent decades great interest was shown towards renewable technologies and, amongst those, wind energy certainly has a special place in terms of potential. One of its biggest advantages is its falling cost of electricity which nowadays competes with traditional technologies, especially when onshore wind energy is considered. For this reason and for its sustainability, governments all around the world have pushed for its massive installation which, for onshore wind, has enabled its capacity to increase from about 178 GW in 2010 to 836 GW in 2022 [2].

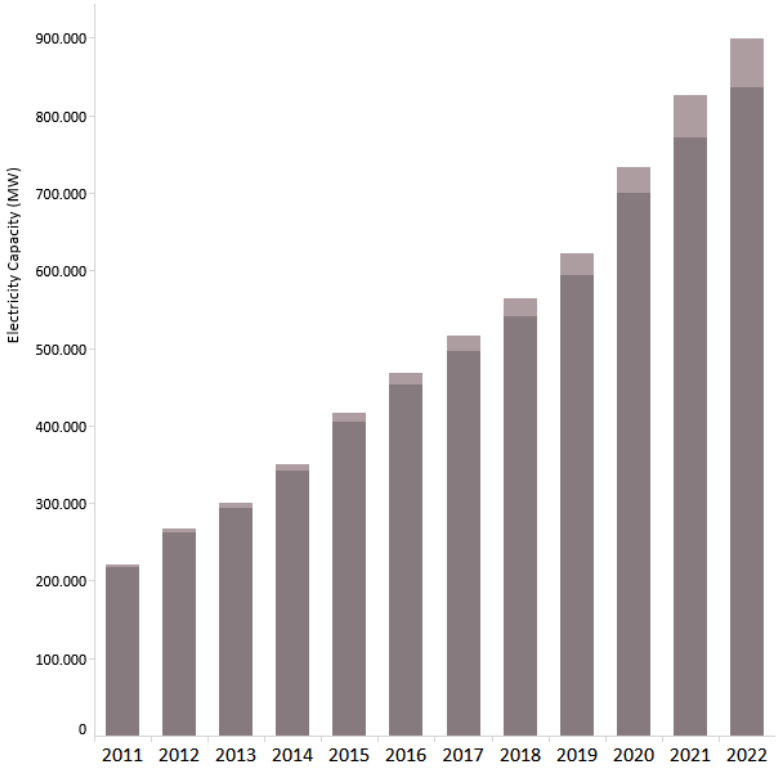

Figure 1.1: Wind energy cumulative capacity 2011-2022. Light grey refers to offshore wind energy while dark grey is onshore [2].

This trend does seem to continue as countries keep on investing money into wind farm projects like France's Les Moulins de Lohan wind farm which will have an installed ca-

pacity of 65 MW or the Netherlands' Maasvlakte 2 which will add another 116.7 MW to Europe wind energy capacity.
In order to reduce further installation, grid infrastructure and maintenance costs wind turbines are often grouped together in a small region. While this clustering choice is beneficial for economics [3, 4] it has a negative effect on the power production of the whole wind farm, that is the power loss due to downstream turbines being partially or completely immersed in the wake generated by the upstream ones. This, in turn, causes both a reduction in the average wind speed and an increase of the turbulence intensity perceived by the downstream turbine which respectively induce a loss of power and increased fatigue loads. The amount of loss of power, while depending on the particular wind farm layout, can reach up to 23% of total power generation [5] and as such it is an interesting chance for improvement.
The most discussed solution to this problem is referred as Active Wake Control (AWC) and it relies on two fundamental strategies: wake redirection and axial induction control. Both of them shift the focus of performance optimization from the single turbine to the whole wind farm.
The first one takes advantage of the fact that when the rotor plane changes direction the wake is steered in the opposite direction and so potentially further from downstream turbine. While effective this method increases the loads on the upstream turbine and as such it must be carefully controlled.
The second one aims at generating a less turbulent and more energized wake by reducing the axial induction factor of the upstream turbine via pitch control. This results in a reduction of both power extracted and its aerodynamic loads while ensuring a greater energy potential for the downstream turbine. The two methods are quite often applied together in order to get both positive effects without exceeding ultimate loads on the upstream turbine.
This thesis is based on two another theses [1, 6] in which potential benefits of AWC were evaluated for a large variety of scenarios. The results were convincing enough and while they considered the AWC impact on ultimate and fatigue loads of the upstream turbine, they did not take into account a potential shortening of the life of the downstream one due to fatigue loads. The work presented here aims at closing this gap by providing a method for assessing the damage on the downstream turbine with a limited amount of aeroelastic simulations.

1.1. Objective and innovative content

While the idea behind AWC is simple, its evaluation is much more complex due to the interaction of the rotor and the turbulent wake which is regulated by dynamic and directional phenomena such as wake meandering or wake superposition. As such simple models cannot capture the full scale of this and a great number of aeroelastic simulations are necessary.
One of the most common approaches [7, 8] to evaluate fatigue loads for a turbine immersed in a wake is to build a lookup table (LUT) containing fatigue loads for a variety of environmental and operational conditions by running a large number of aeroelastic simulations. The fatigue damage for a new condition is then calculated by interpolating on the LUT.
An alternative approach was recently proposed by Bossanyi [9] in which loads contributions of different causes are calculated separately and combined together later.
The approach adopted in this work strays a bit from the ones mentioned, mainly because it maps any control change of the upstream turbine via yawing or derating to the steady state wake that forms behind it. To do this a set of initial operational and environmental conditions are chosen and run in very fast steady state wind farm engineering model [10] which can provide the properties of the steady state wake in a very short time for a considerable number of cases. These, along with information about the turbulence intensity in the wake, are then combined to create a reduced set of conditions which are simulated in Cp-Lambda, an aeroelastic software developed in PoliMi [11]. Finally the results of the simulations can be used to describe the initial set of conditions to build the fatigue constraint curve which, could be coupled with the ultimate loads constraint curve of the previous thesis [1] to provide a generalized framework to approach the AWC problem.

1.2. Thesis outline

The thesis will be structured as follows. Chapter 2 will provide a general description of a wind turbine wake as well as of the methods commonly used to limit its effects. This is useful to comprehend the choices made later in the modeling section and why there is so much interest in AWC. Chapter 3 will be focused on detailing the wind farm structure considered, how the wake is modeled throughout the work and describing the software employed for simulations of wake interactions with the farm. The work proceeds by using this information to present the overall methodology of assessing fatigue loads of the downstream turbine in Chapter 4. Within it the steady state wake modelled in the engineering wind farm model is parametrized for a number of various scenarios and the

relevant cases to be simulated in the aeroelastic tool are selected in order to construct the fatigue loads constraint curves. Finally, in Chapter 5, results will be presented starting from the fatigue loads dependence of operational and environmental parameters, moving on to the overall constraint curves for different downstream lateral offset. Lastly, in Chapter 6, conclusions will be drawn over the implication of the results and the reliability of this approach. A section will also be dedicated to future developments and possible improvements on the work presented.

2 | Wind Farm Analysis and Control

2.1. Turbine-wake interaction

When extracting energy from the wind, a perturbation in the wind itself is unavoidable since it has to be pushed back in order to push the turbine. The wake that forms downstream of the turbine will be then characterized by lower wind speeds and a stronger turbulence compared to free flow.
Conventionally, the wake is divided into three regions which are referred to as near, intermediate and far wake[5, 12, 13].
In the near wake, which usually spreads from two to three rotor diameters downstream, the flow is characterized by the relaxation of axial and radial pressure gradients due to the extraction of momentum by the rotor. These gradients, and as such the wind speed deficit and the added turbulence themselves, are proportional to the thrust coefficient of the turbine. Furthermore in this region additional "mechanically" generated turbulence due to tip vortices shed by the blades and due to the wind interaction with the nacelle and the tower are present. Normally this turbulence is dissipated in the near wake and no trace of its periodicity is found further downstream.
As the wake moves downstream in the intermediate wake region, the wind speed gradient between the free flow and the wake causes shear generated turbulence that re-energizes the center of the wake while expanding the area of influence of the wake that becomes wider and shallower.
Lastly in the far wake, beyond about five rotor diameters downstream, the wake enters a state of self similarity and a axysimmetric 3D Gaussian function can be used to approximate the wind profile. This can be done since the shape of the profile of both the mean wind speed and turbulence is constant and only its peak and width dimensions must be adjusted as the wake proceeds downstream.

As with all problems where turbulence is involved, the interaction between the wind flow

and the rotor is highly complex and depends on variety of environmental and operational parameters. Aside from the features mentioned above a wake can also be characterized by other phenomena such as wake superposition if multiple wakes are interacting or wake meandering if the length scale of eddies in the atmospheric turbulence is greater than two rotor diameters[14].
In any case the rotor under wake effects is subject to non-homogeneous flow which on average has a lower mean wind speed and a higher turbulence compared to the free flow. This will respectively cause a reduced power output and possibly faster and broader variation of loads, increasing fatigue damages to the wind turbine structure.

2.2. Wind Farm control based on yaw and derating

For the reasons explained in the previous section it is clear why great interest was shown towards wind farm control strategies oriented at reducing the impact of wake effects. All of them are based on worsening the performances of the upstream turbine in order to improve the downstream turbine's ones. In this framework performance means both power production and loads.
Amongst several wake control strategies, two are of particular interest: wake redirection and axial induction control. While they can be applied independently, benefits are maximized if they are coordinated as it will be clear after a brief explanation of the two methods.

2.2.1. Axial Induction control

This technique relies on controlling the axial induction factor a by acting on either the pitch angle of the blades or the rotor rotational speed of the upstream turbine. The effects are mainly two: firstly reduction of wake deficit and wake added turbulence since the wind is less slowed down; secondly a decrease in the overall loads perceived by the turbine since the thrust coefficient C_T is related to a with the following equation:

$$C_T = \begin{cases} 4a(1-a)F, & \text{if } a \leq \frac{1}{3} \\ 4a(1-\frac{1}{4}(5-3a)a)F, & \text{if } a \geq \frac{1}{3} \end{cases}$$

if, for example, Glauert correction model is employed where F is Prandtl's tip loss correction.
By reducing a the upstream turbine will also extract a reduced power from the wind, hence why "derating" is also used to describe this strategy, but the downstream will have

effectively more wind energy available. Axial induction control alone is rarely enough to make a significant difference in power production but it is nonetheless interesting because of its load reduction potential and, as such, it is considered a "safe" way to control wake effects.

2.2.2. Wake Redirection

Wake redirection exploits the fact that when the rotor axis is misaligned with the main wind speed direction then lateral forces occur and the wake can be steered away from the downstream turbine. This misalignment can be produced through either a yaw or a tilt angle, though usually the former is employed. Clearly the upstream turbine will again

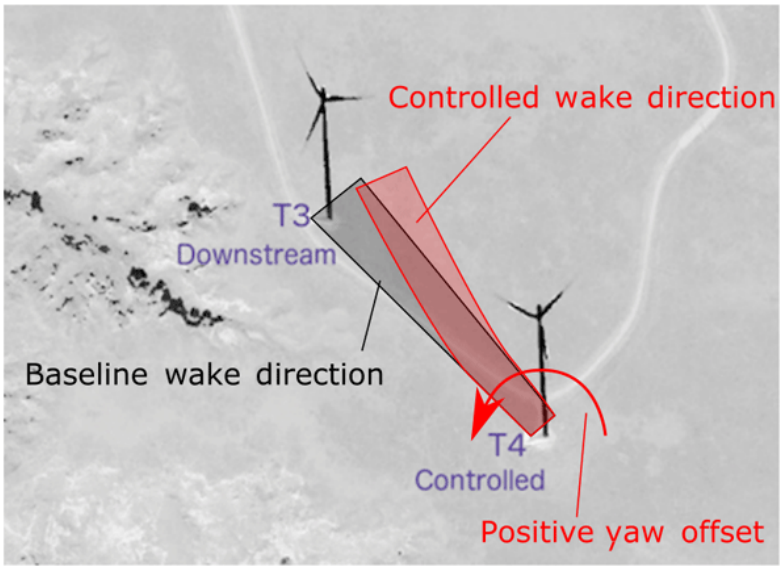

Figure 2.1: A scheme of wake steering through yaw control. Credits to Fleming et al[15]

produce less power but it will also be subjected to higher loads compared to the ones measured during the design process. The advantage compared to axial induction control is that the potential power gain for the downstream turbine is much higher since, if done right, the turbine itself will be out of the wake.
Nonetheless because of the increase in loads magnitude for the upstream turbine, this strategy has also potentially greater risks of shortening the life of the machines involved and as such its impact in general must be carefully evaluated. Starting from Dadda's results [6], the fatigue loads for the upstream turbine are not limiting and usually decrease during AWC as it can be seen in Figure 2.2. For this reason, in this thesis only the impacts on the downstream turbine will be evaluated.

As it can be seen from the same figure yaw based wake control has an added layer of

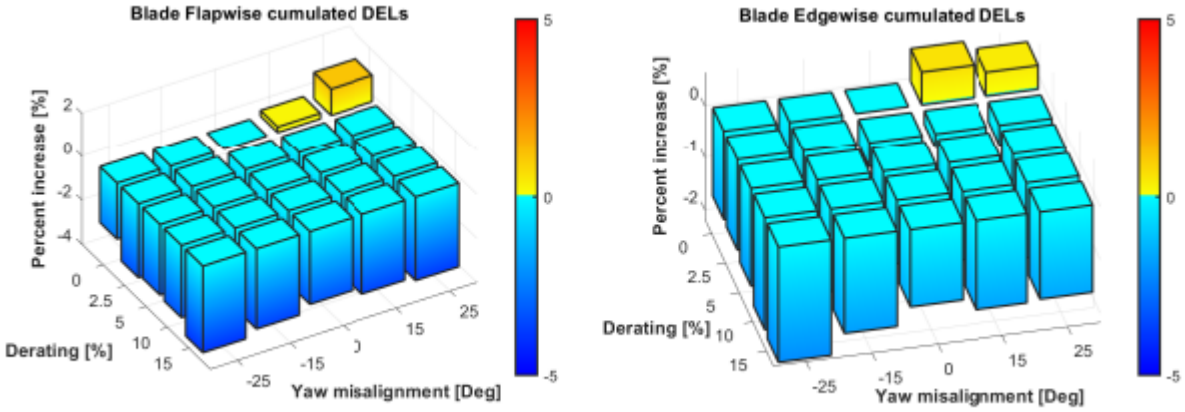

Figure 2.2: Flapwise and edgewise cumulated DEL variation as a function of yaw misaglinment and derating with AWC turned off at wind speeds above 15 m/s [6]

complexity through its asymmetry over the no control condition. This happens because of the wake's natural swirl due to the rotation of the rotor which by itself gives already some degree of steering to the wake in one predominant direction so an additional steering due to yaw based control will cause asymmetric behaviour that may be harder to predict. The coupling between the two different control methods is symbiotic since it can achieve at the same time:

- a more energized and less turbulent flow perceived by the downstream turbine
- loads for the upstream one that are comparable with the baseline case
- an increase in the power extracted by the overall wind farm

3 | Wake Modelling

3.1. Reference wind turbine and farm

A simple wind farm consisting of two DTU-10 MW [16] wind turbines will be considered for this thesis. The choice of this particular machine is due to both reasons of continuity with previous works [1] and of availability of data. Furthermore the DTU-10 MW is often found in literature and as such it is an ideal choice in a cross-comparison perspective.

Propriety	**Value**
Class and category IEC	Class 1A
Rated Power	10 MW
Rotor orientation, configuration	Upwind, 3 blades, clockwise rotation
Control	Variable speed, collective pitch
Rotor diameter	178.3 m
Hub diameter	5.6 m
Hub height	119 m
Cut-in wind speed	4 m/s
Cut-out wind speed	25 m/s
Rated wind speed	11.4 m/s
Minimum rotor speed	6 rpm
Rated rotor speed	9.6 rpm
Drive-train	Medium speed, multiple stages gearbox
Gearbox ratio	50
Rated tip speed	90 m/s
Rotor mass	228 tons
Rotor overhang	7.1 m
Nacelle uptilt	5°
Rotor precone	4.65°

Table 3.1: DTU 10 MW reference turbine main parameters.

The machine was developed by DTU starting from the NREL 5 MW, upscaling its features while taking into consideration the new generation of large scale wind turbines. The

#	Airfoil	Thickness [%]	Twist [deg]	Spanwise position [%]
1	Cylinder	100	14.50°	0
2	Cylinder	100	14.50°	1.74
3	FFA-W3-480	48	10.08°	20.8
4	FFA-WE-360	36	7.3°	29.24
5	FFA-WE-301	30.1	5.75°	38.76
6	FFA-W3-241	24.1	0.1°	71.78
7	FFA-W3-241	24.1	-3.43°	100

Table 3.2: Airfoil properties for the DTU 10 MW turbine

turbine's main features are reported in Table 3.1, while properties of airfoils on which the blades are based can be read in Table 3.2.
The downstream distance separating the two wind turbines in the farm is equal to 5 rotor diameters (D) for all cases hereby considered while the lateral distance can vary between -0.5D and +0.5D in order to take into account the effects of different wind directions.
Additionally for this thesis only the upstream turbine will be yawed or derated since an active control on the downstream one would complicate the problem too much from a computational point of view.
Obviously this configuration is simple and not sufficient to evaluate fatigue loads in a real wind farm since, by its nature, it bypasses phenomena related to interactions between wakes of different turbines. Nonetheless it should be considered a possible starting point for a more complex model that could be developed in the future.

3.2. Wind turbine modeling through multibody software Cp-Lambda

In order to compile the wake-properties-based-LUT a set of relevant aeroelastic simulations were run through the use of Cp-Lambda, an aero-servo-hydro-elastic code developed by DAST-Polimi[11]. The code is multibody-based, meaning that components of the wind turbine can be modelled with different standard elements (rigid bodies, flexible beams, joints, sensors, actuators, springs, dampers.) and combined depending on the particular machine that is being studied. An example of the modelling of a wind turbine can be seen in Figure 3.1. Cp-Lambda is based on blade element momentum and annular stream tube theory and it can take into account several aerodynamic effects such as wake swirl, tip and hub losses, unsteady corrections and dynamic stall. The code received as inputs, aside from data of the wind turbine, full field time series generated by TurbSim[18]. As it will be more thoroughly explained in chapter 3.4 it is exactly through the modification

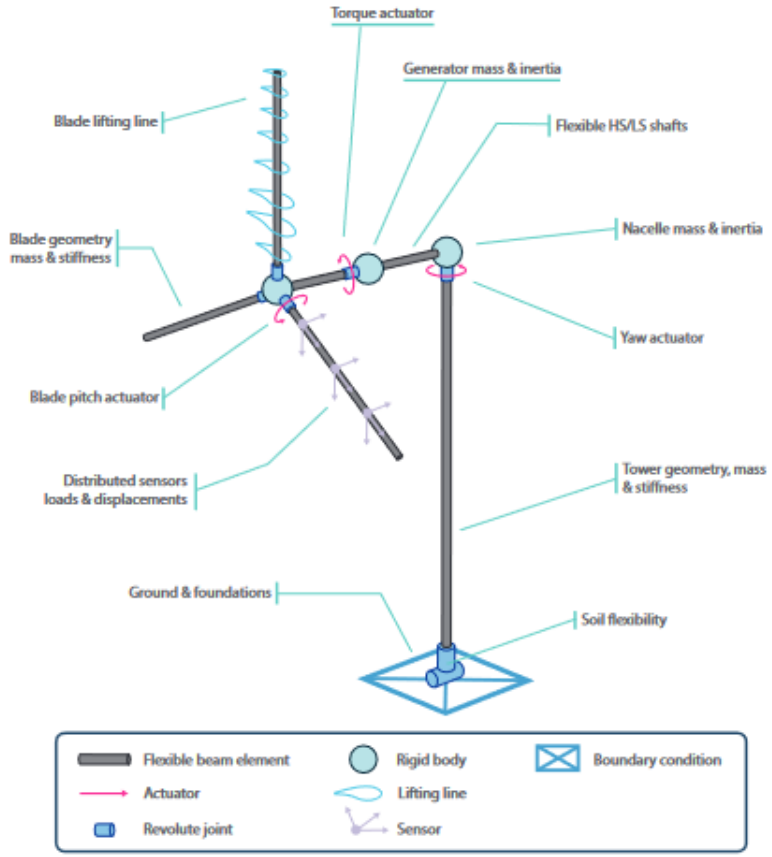

Figure 3.1: Topological description of a wind turbine in Cp-Lambda[17]

of these files that the wake effects on the downstream turbine will be implemented. It is however worth to note here that to the time series files generated, Cp-Lambda then attaches 50 initial seconds of constant wind speed in order to reach a quasi-steady state condition and prepare the wind turbine for the actual inflow that is subject to the study. Cp-Lambda then returns as an output, amongst other quantities, time series of forces and moments of predefined sensors of particular interest. The sensors taken into consideration in this work are the blade root edgewise and flapwise bending moments and the tower base side to side and foreaft bending moments.

3.3. Wind farm modeling through FLORIS

FLOw Redirection and Induction in Steady State (FLORIS) is a tool developed by the NREL in cooperation with Delft University of Technology with support from the U.S. Department of Energy Wind Energy Technologies Office. The software, through steady state wake models, enables rapid computations of wind farm operating points and their

optimized yaw misalignment setpoints for a variety of operational and environmental conditions. As such it is a very powerful tool in the active wake control framework and can return scientifically interesting results in a short time[19].
In FLORIS a wake model is composed by four submodels that together constitute the wake:

- Wake deficit: it regulates the deceleration of the flow caused by momentum extraction.
- Wake deflection: it controls how the wake is steered when a yaw misalignment between the rotor and the main wind direction is introduced.
- Wake turbulence: it describes the degree of turbulence the area affected by the wake is subjected to.
- Wake combination: it models how two wakes interact with each other. This is more interesting for more complex wind farms than the one taken into consideration during this thesis.

For this thesis, the tool is mainly used as a calculator of the steady state properties of the wake generated by the upstream turbine. These properties will then be used to engineer the inflow necessary for Cp-Lambda. Most notably the wake deficit will be modelled as Gaussian with A as the peak, σ as the standard deviation and (y_c,z_c) as the coordinates of the center of the wake in a reference system centered at the rotor hub of the downstream turbine.
For full disclosure FLORIS v3.0 available for Python is employed and the wake models considered are summed up in Table 3.3.

Submodel	Name
Deficit	Gauss
Deflection	Gauss
Turbulence	Crespo & Hernandez
Combination	Sum of Squares Freestream Superposition

Table 3.3: Wake models employed in FLORIS

3.4. Definition of waked inflow for multibody software

The steady state properties of the wake calculated by FLORIS are then used to generate inflow time series that resemble the conditions in which the downstream turbine will operate. For each case to be simulated in Cp-Lambda two time series are generated by TurbSim with the same mean wind speed, same random seed but different turbulence intensities: one is relative to the freestream turbulence and one to the turbulence inside of the wake region. An example of the wind speed time profile is reported in Figure 3.2.

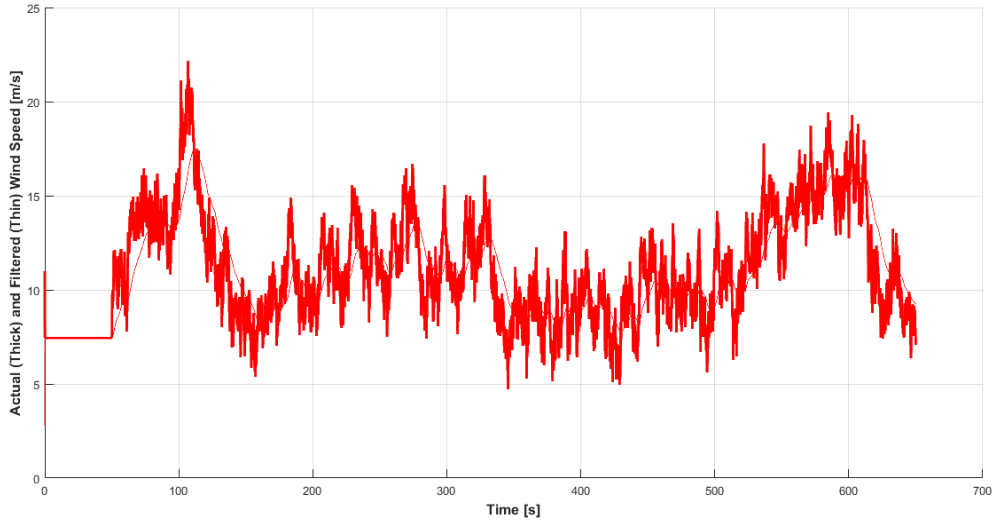

Figure 3.2: Wind speed time history at the hub for V_m=11 m/s. The constant value of the first 50 seconds is needed for the software to achieve quasi-steady state conditions before the actual simulation starts.

The freestream turbulence is evaluated as a pure function of wind speed and of the class of the wind turbine as from the standard IEC-61400; its trend compared to wind speed can be observed in Figure 3.3.
For the wake region, the wake added turbulence approach is used instead. It involves the calculation of a parameter called added turbulence I_{add} through empirical correlations that are usually functions of the thrust coefficient C_T, the downstream distance with respect to the rotor along the main wind direction x and the ambient flow turbulence intensity I_0. The wake turbulence intensity I_w is then found as:

$$I_w = \sqrt{I_0^2 + I_{add}^2} \tag{3.1}$$

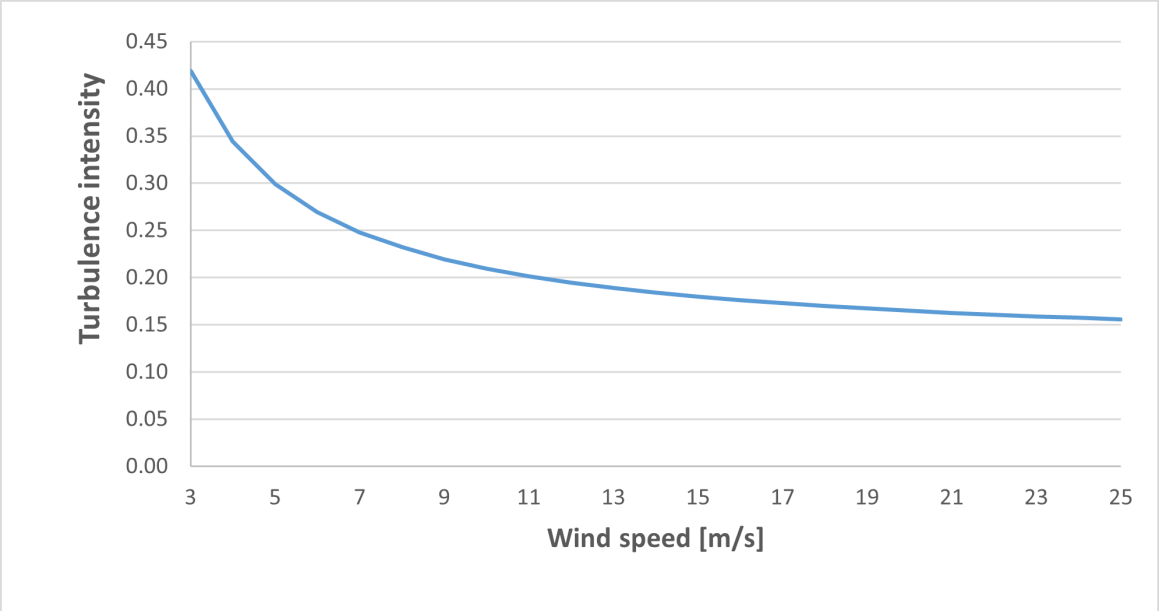

Figure 3.3: Ambient turbulence as a function of mean wind speed

Past the near wake region, it was found that the added turbulence intensity can be assumed axysimmetric and self similar in the cross sections [20] and multiple 3D models for it were then developed [21, 22]. The generic shape of added turbulence intensity cross section at fixed downstream distance can be observed in Figure 3.4. It has a local minimum in the center of the wake and reaches the global maximum at one rotor radius from it before approaching zero at a sufficiently large enough distance.

In this work a 1D, maximum wake added turbulence approach is used for simplicity but a more complex distribution could be adopted without a substantial increase in computational burden; it would just imply the generation of more TurbSim time series, one more

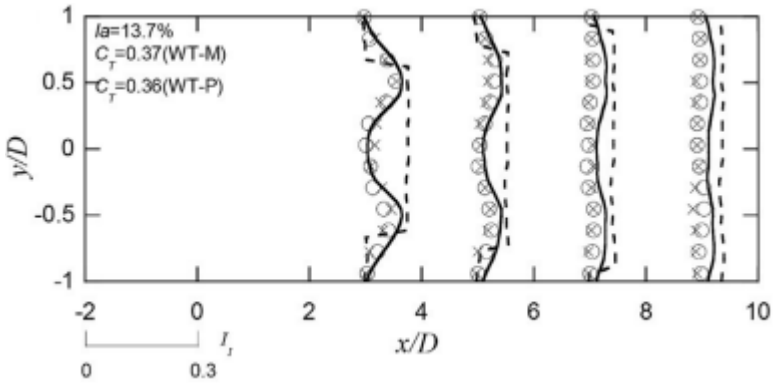

Figure 3.4: Ishihara model[22] of added turbulence (black line) and added turbulence from LES (crosses and circles)

for each turbulence intensity considered.
The correlation for the maximum wake added turbulence employed here is the one derived by Quarton and Ainslie in [12]:

$$I_{add} = 4.8 C_T^{0.7} I_0^{0.68} (\frac{x}{x_N})^{-0.57}$$

where x_N is the estimated length of the near wake which using the definition by Vermeulen [23] is

$$x_N = \frac{\sqrt{0.214 + 0.144m}(1 - \sqrt{0.134 + 0.124m})}{(1 - \sqrt{0.214 + 0.144m})\sqrt{0.134 + 0.124m}} \frac{r_0}{dr/dx} \tag{3.2}$$

where

$$m = \frac{1}{\sqrt{1 - C_T}}$$
$$r_0 = R\sqrt{\frac{m+1}{2}}$$
$$dr/dx = \sqrt{(\frac{dr}{dx})^2_{amb} + (\frac{dr}{dx})^2_{sh} + ((\frac{dr}{dx})^2_{mec}}$$
$$(\frac{dr}{dx})_{amb} = 2.5 I_0 + 0.005$$
$$(\frac{dr}{dx})_{sh} = \frac{(1-m)\sqrt{1.49 + m}}{9.76(1+m)}$$
$$(\frac{dr}{dx})_{mec} = 0.012 B \lambda$$

R is the rotor radius, B is the number of blades, λ is the rotor tip speed ratio.
Practically C_T should be a function of both the mean wind speed and the operating conditions of the turbine (mainly yaw misalignment and derating value). In order to simplify the problem to be able to describe the wake effects only in terms of ambient wind speed and gaussian steady state wake deficit, the influence of derating and yaw misalignment is here neglected. Since by increasing the misaglinment or the derating value, C_T and as such I_{add} would decrease, the added turbulence is then always calculated by using yaw misalignment and derating equal to zero, corresponding to the uncontrolled scenario. This way even if the wake model is not completely accurate it is at least conservative. Additionally since the added turbulence parameter is then weighted with the ambient turbulence through Equation 3.1 a small variation due to operating conditions does not propagate too much to the final wake turbulence value, especially for low mean wind speeds which are characterized by high I_{amb}.
The turbulence intensity trend, function only of V_m, is then summarized in Figure 3.5. As

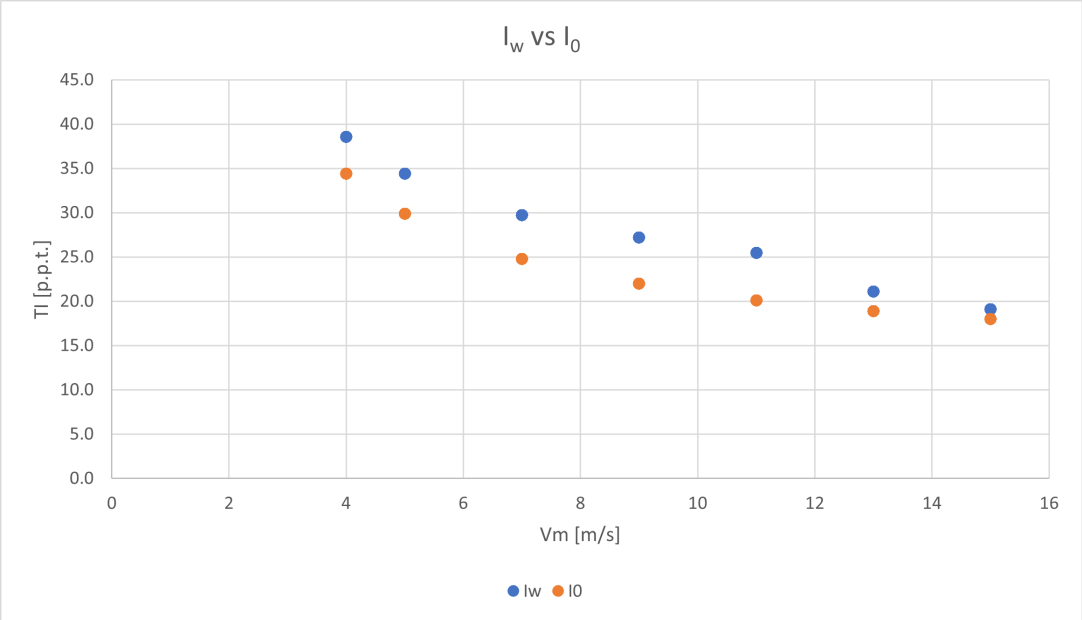

Figure 3.5: Comparison between ambient and wake turbulence intensities as a function of V_m

it can be seen the turbulence intensity increases of about 5% in the wake for wind speed lower than rated, after that, because of the lower C_T, the difference between ambient and wake TIs is much more limited.

After generating the two TurbSim files they can finally be combined to describe the waked inflow blowing on the downstream turbine. To do that the 11x11 wind grid of width and height equal to 180 m is divided in two regions:

- out-of-the-wake region which is described by the ambient turbulence time series as it is
- in-the-wake region which is built by superimposing the Gaussian steady state wake deficit that FLORIS returns with the increased turbulence time series

One grid point is considered to be in the wake region if either the wake deficit in that point is greater or equal than 0.2 m/s or if the distance from the center of the wake is more than 1.48 standard deviations σ used to describe the width of the gaussian wake. The first condition is there simply because wake deficits greater than 0.2 m/s are not considered relevant enough for this study. The second one is due to the fact that 1.48σ is the distance at which the gaussian function assumes a third of its peak value. This was done to make sure that the added turbulence region always extends further enough from the point of maximum turbulence intensity, which is typically at rotor radius distance from

the center of the wake, but not too much into the free stream. This was also a compromise between an excessively conservative choice of considering the maximum added turbulence everywhere the wake has turbulence effects and the unsafe one of increasing the wake turbulence only up to one rotor radius from the center of the wake.

4 | Methodology for assessing fatigue loads of downstream turbine

In this chapter the overall methodology for the construction of the look up table will be introduced. Firstly a set of initial environmental and operating conditions for the upstream turbine is selected and then run in FLORIS to extract the steady state properties of the waked inflow. The wake is thus parametrized and its properties are then binned in order to restrict the number of cases to be actually simulated in the aeroelastic software. The loads histories are then postprocessed and so the fatigue loads are obtained as a function of the steady state wake properties. In particular to characterize fatigue, the concept of damage equivalent loads (DELs) is employed. This is merely an approximation for a twofold reason:

- local effects are not considered, only an equivalent load at the blade root or at tower base. In actual application the distribution of the loads is also important
- DEL computation involves the ranges of the load's cycles but not their mean values

While simplified, this approach enables, through a fast software such as FLORIS, to map the operating conditions of the upstream turbine to the steady state wake properties and then to the loads of the downstream turbine. The great strength of this framework is, if reasonable, its scalability, since FLORIS could easily handle a more complex wind farm, bypassing the need of full scale aeroelastic simulations. In a more generalized approach the LUT would also be function of the operating conditions of the downstream turbine if AWC would be applied to it as well but this does not invalidate the overall idea of this thesis.

4.1. Parametrization of the wake

Before illustrating how the steady state wake properties are recovered from FLORIS, it is useful to estabilish the domain in which the set of simulations are run.
The environmental and operating parameters of the wind farm selected are:

- wind speed: indicated as V_m, it is the mean wind speed at hub height. It is measured in [m/s] and varies in [4 5 7 9 11 13 15]. This range is chosen since it has the most potential for AWC as above 15 m/s the wake is already energized enough that the power gain would be uninteresting. Furthermore, as Dadda [6] found, loads constraints may become too strict for the upstream turbine above 15 m/s.
- yaw misalignment: it is the angle of misalignment between the main direction of the wind and the rotor. It is measured in [°] and varies in [-25 -15 0 15 25] where positive means counter-clockwise rotation. This range is chosen mainly because of continuity with previous theses, nonetheless yaw misaglinments greater than the ones reported are not interesting from a practical standpoint.
- derating: it is the reduction, in percentage, of the power coefficient C_P compared to the optimal one. It varies in [0 2.5 5 10 15] %. This range is also chosen because of continuity with previous works.
- lateral offset of the downstream turbine: it is the lateral displacement, measured in rotor diameters, from the line parallel to the wind direction that passes through the upstream turbine. It varies in [-0.5 -0.25 0 0.25 0.5] D where positive means to the left when facing the upstream turbine upfront. The lateral offset carries the information about wind direction, as two wind turbines in a farm will directly overlap only with a specific wind direction. This parameter was considered in this study to evaluate if AWC may be interesting for situations in which the downstream turbine is not completely immersed in the wake by default.

Furthermore, for each case, the ambient turbulence intensity is considered a function of the mean wind speed as in Figure 3.3.
By considering the combinations of this parameters a total of 875 cases are then simulated in FLORIS in order to extract trends and range of variations of the steady state wake properties.
While FLORIS allows to change the farm layout, wind conditions and yaw misalignments very easily, to implement the degree of derating one has to modify the input files containing wind turbine specifications. In particular FLORIS requests the power coefficient C_P and thrust coefficient C_T as a function of V_m. These values are obtained by reducing the

optimal power coefficient calculated by Cp-Lambda by the set of derating values before mentioned. In this work constant tip speed ratio derating was employed, meaning that the change in power and thrust coefficient are achieved by an increase in the pitch angle of the blades. This operation is carried out through a MATLAB routine that, from the C_P vs TSR vs Pitch curves calculated beforehand, finds the pitch angle, and the turbine setpoint, needed to obtain, at fixed TSR, the reduced C_P. An example of this regulation can be seen in Figure 4.1.

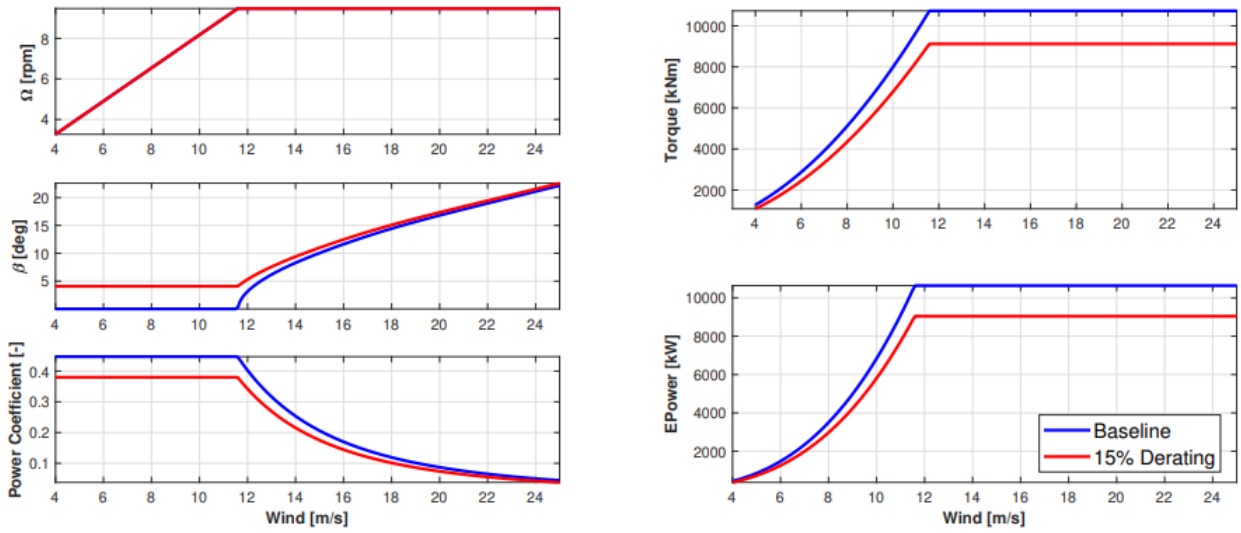

Figure 4.1: An example of the operational setpoints obtained from derating at 15% compared to the baseline case [6]

4.1.1. Gaussian fitting

For each one of the 875 cases, which will be thereafter referred to as "initial cases", the steady state wind speed is then extracted at 5D downstream through the FLORIS function `calculate_cross_plane` to obtain a field that looks like the one in Figure 4.2. As it can be seen the field is composed by two main contributes: the shear profile and the wake. To isolate the latter, the former is subtracted by using the shear profile power law:

$$\frac{u}{u_{hub}} = (\frac{z}{z_{hub}})^{\alpha}$$

where u_{hub} and z_{hub} are respectively the wind speed along the main direction at hub height and the hub height itself, z is the vertical coordinate and alpha is the shear coefficient which for all cases considered is fixed at 0.12. Through this difference the mean wind speed at each height is removed to highlight the steady state deficit due to the wake.

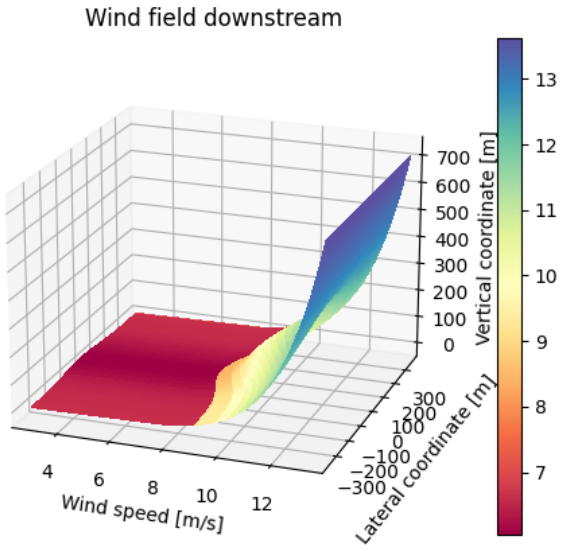

Figure 4.2: Wind field at 5D downstream with V_m=11 m/s

The result of this operation can be seen in Figure 4.3. What remains of the original wind field is then numerically fitted in a 2D gaussian function:

$$\delta(y,z) = A\exp^{-(\frac{(y-y_c)^2}{2\sigma^2}+\frac{(z-z_c)^2}{2\sigma^2})}$$

where δ is the wake deficit, A is the maximum deficit at the centre of the wake, y_c and z_c are respectively the lateral and vertical coordinate of the centre of the wake and σ is the standard deviation of the gaussian. By employing this procedure each one of the 875 initial cases is then characterized by a set of steady state wake properties. From now on, A, σ y_c and z_c will be the quantities we refer to when mentioning steady state wake parameters.

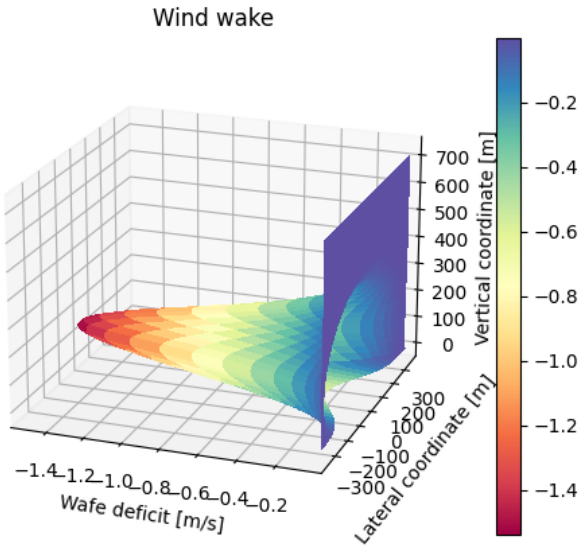

Figure 4.3: Wake deficit at 5D downstream with V_m=11 m/s

4.2. Analysis of the cases to be simulated for fatigue evaluation

In this section an overview of the wake parameters obtained from the simulation of the initial cases run in FLORIS will be presented, analyzing their correlation with the upstream turbine operative condition and the one amongst them. Starting from there the methodology for the selection of the significant cases will then be defined.

4.2.1. Steady state wake parameters analysis

For the initial cases considered the range of variation is much more significant for σ, A and y_c while not as much for z_c as it may have been expected from the fact that the wake control techniques employed here do not act on the vertical position of the wake (as tilt-based steering might do) and as such z_c is always in the vicinity of hub height. More specifically it varies in the range [128 145] m and, while it also depends on yaw misalignment and derating values, it mostly related to V_m variations as can be seen in Figure 4.4. Because of its limited variation this parameter's influence over the fatigue loads will not be considered in this study and, instead, the median of the range, equal to 133.42 m, will be employed for all the cases to be simulated in Cp-Lambda.

The maximum deficit of the gaussian wake A mostly depends on both V_m and the de-

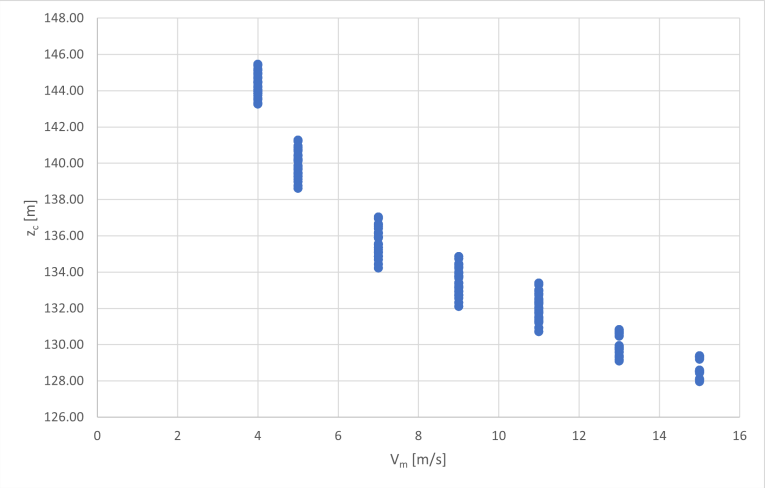

Figure 4.4: Scatter plot of the initial cases' z_c against V_m

rating degree while yaw misalignment, while always beneficial in reducing its intensity, has a negligible amount as it can be seen in Figure 4.5. By inspecting the figure a very noticeable trend appears: the maximum wake deficit increases as the wind speed increases up to the turbine rated speed after which, as a result of pitch regulation, the thrust coefficient decreases and the wake deficit with it. Naturally, by increasing the derating of the machine, the wake deficit decreases as a response of the reduced C_T, however it can be seen that the most significant effects are obtained at intermediate wind speeds when A is not low enough already because of low V_m or when C_T is high enough that a small percentage variation of it can actually have an effect on the wake.

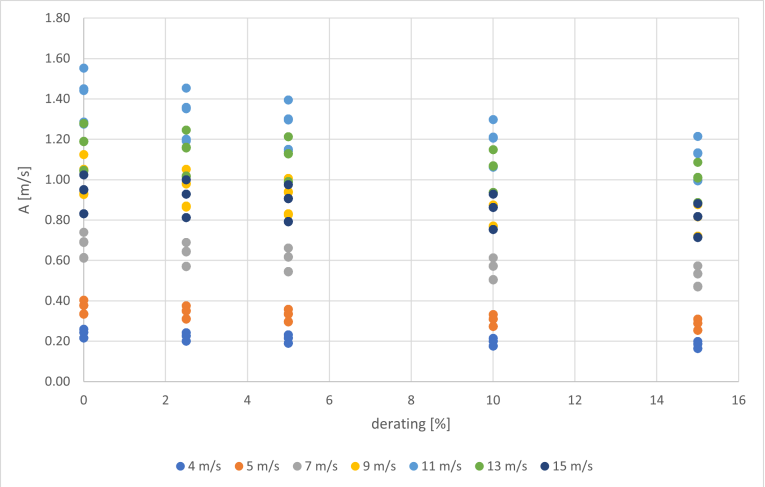

Figure 4.5: Scatter plot of the initial cases' A against V_m and the derating degree

For σ variations the most influential parameter is V_m by far while the derating degree has a weak impact and yaw misalignment has a pretty much non existent influence on it,

see Figure 4.6. As wind speed increases the wake's area of influence shrinks as a result of the impact of the ambient turbulence intensity which decreases with V_m. As a matter of fact a less turbulent free flow facilitates energy recovery in the wake since the wake effectively interacts with a more energized and stable source of wind. This is also the reason why derating is beneficial to the shrinkage of the wake even if in a less evident way. As the thrust coefficient is reduced the effective turbulence in the wake and in its vicinity is reduced as well, once again aiding energy recovery in the middle of the wake and limiting its expansion.

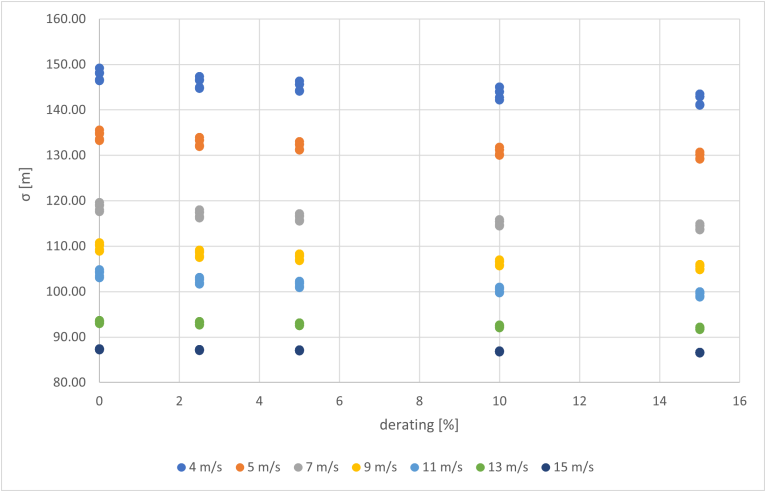

Figure 4.6: Scatter plot of the initial cases' σ against V_m and the derating degree

Lastly y_c dependence on V_m and the yaw misalignment can be seen in Figure 4.7. Clearly for this wake parameter the most important factor is how much the rotor is steered since it influence the intensity of the lateral component of the thrust forces that the wind encounters, however derating also plays a role. As the derating degree increases the thrust forces are reduced and as such the wake will be steered with a lower efficacy. This is also evident by looking at how the lateral deviation is limited for wind speeds above rated value. Notably this is one of the weaknesses of the combination of wake steering and derating: as the derating degree of the upstream turbine increases, some benefits of wake steering are hindered.

It is also worth noting that the lateral steering of the wake is always very limited and it reaches at best about a fourth of the rotor diameter's length. This is both due to the fixed downstream distance of 5D and to the high turbulence intensities of the 1A wind turbine category which obviously reduce the steering effect. As such for different conditions to the ones considered and these values could change significantly.

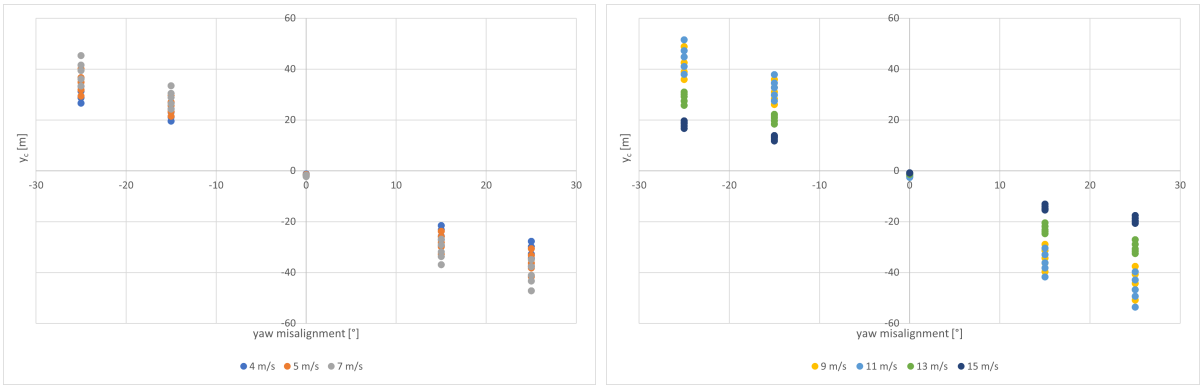

(a) (b)

Figure 4.7: Scatter plots of the initial' cases y_c against V_m and the yaw misalignment angle, separated for low and high wind speeds for readability

4.2.2. Selection of significant cases

To understand how the significant cases were selected it is necessary to first analyze how the wake parameters are correlated amongst themselves and most notably how the maximum deficit A and the gaussian standard deviation σ are related. By looking at Figure 4.8 their relationship can be envisaged: each stripe of points is representing a set of initial cases with the same V_m, with increasing values of V_m by moving from right to left; the proportionality between A and σ is then very clearly inverse for $V_m < V_{m,rated}$ and direct elsewhere.
The consequence of this is that, to an extent, wakes that are characterized by a wide and deep or narrow and shallow gaussian functions, are not really physical and can be excluded. This is the clear advantage of basing the look up table on the properties of the steady state wake properties: as their domain is limited, the number of aeroelastic simulations can be reduced significantly as well.

Starting from this concept, the domain of the steady state wake properties, mainly A, σ and y_c, is gridded into an equispaced 5x5x5, obtaining as such for each wake parameter 4 possible bins. Obviously a greater amount of bins is possible and recommended for more precise results but for this study these numbers were considered acceptable to test the methodology proposed without having to run thousands of aeroelastic simulations.
For each initial case run in FLORIS an operation is then carried out, that is the binning of the steady state wake properties into this grid. Each initial case will be then described by a combination of the bins and its mean wind speed which in actuality means that to fully characterize it by interpolation $2^3 = 8$ cases will be needed to be simulated in Cp-Lambda as can be seen in Figure 4.9, since there are three wake parameters. Each

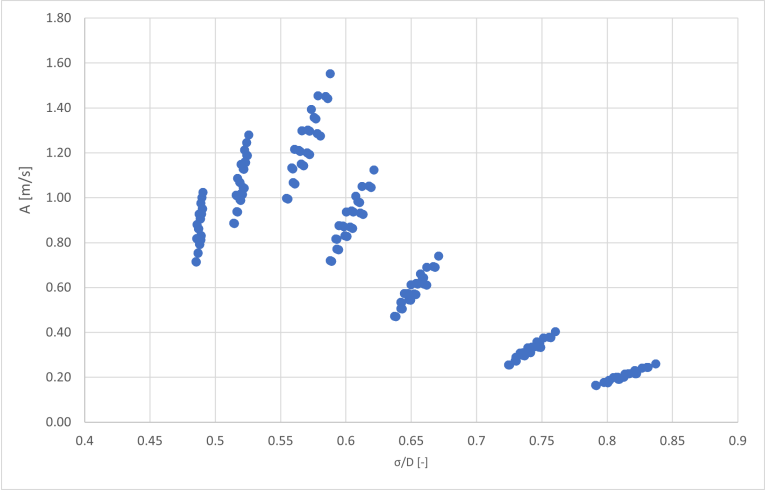

Figure 4.8: Correlation between A and σ for the initial cases

one of this 8 cases will be the ones that are significant for the description of that specific initial case and it will be characterized by a wind speed $V_{m,i}$, a maximum wake deficit A_i, a wake width σ_i and a lateral coordinate of the wake center $y_{c,i}$. While this may seem like a large number to be considered for each initial case, the majority of them are in common between different initial cases which, combined with the fact that not all possible combinations of A, σ and y_c are physical cases, brings down the number of significant cases to a reasonable amount.

For this particular choice of number of bins 220 significant cases are obtained, representing 220 different wind inflows that the downstream turbine will experience and that are necessary to be simulated in Cp-Lambda for the construction of the LUT table.

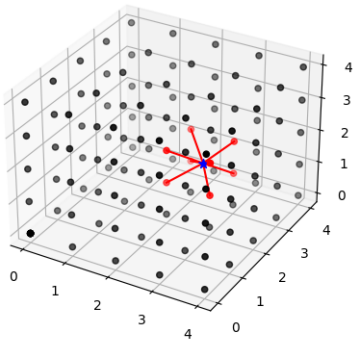

Figure 4.9: Representation of the binning of the initial case and the selection of a significant case. The blue star stands for the initial case while the 8 red dots surrounding it are the significant cases

4.3. Cp-Lambda simulation and LUT construction

Once the significant cases are identified, for each one of them, a 10 minutes wind time series is generated from the steady state wake properties, as described in section 3.4, and fed to Cp-Lambda. The software then simulates the wind turbine response and, through the sensor elements, stores the time history of the loads selected. In particular for this work four loads are considered: blade root edgewise and flapwise bending moments and tower base fore-aft (FA) and side-to-side (SS) bending moments.
For fatigue evaluation the rigorous approach would be to find the most heavily loaded direction for each section of interest, which, in general, is different compared to the two orthogonal directions of both blade and tower root. However since the procedure to find the most heavily loaded direction is time consuming and since for the downstream turbine the yaw angle is always fixed at zero, it was deemed sufficient enough to proceed by considering the four loads as they are.
Once the sensor's reading are extracted, the rainflow analyses are run and the results are binned in a Markov matrix that has 64 rows for the loads' range and 128 columns for the loads' mean values. Finally, the damage equivalent loads (DEL) are then computed as by:

$$DEL = (\frac{\sum_i^n (n_i L_i^m)}{T f_{eq}})^{1/m}$$

where n_i is the number of cycles for the ith range, L_i is the load range for the ith range, m is the exponent of the SN curve and f_{eq} is, according to the Standards, the equivalent frequency corresponding to 10M cycles in 20years ($\frac{1 \cdot 10^7}{20 \cdot 365 \cdot 24 \cdot 60 \cdot 60}$ Hz) and T is the simulation time (in seconds). For the blade root DELs m=10 is taken (glassfiber) while for the tower base DELs m=3 is chosen (steel).
Notably the DELs are not weighted with the Weibull wave function since the approach used in this thesis is aimed both at providing insights for specific wind speeds and at the construction of constraint curves as general as possible and not location-dependent.
This has the downside that the turbine operation is not considered as a whole and, as such, some negative upstream conditions which may balance with a positive one at different wind speeds are not regarded as safe. The obvious advantage is that, in this way, a complete knowledge of the fatigue loads is obtained as a function of the specific environmental and operational conditions.
From the DELs computed a LUT table function of V_m, A, y_c and σ is finally constructed and it can be employed for the characterization of fatigue loads of the initial cases run in FLORIS. Because of the choice of simulating only wakes that are physical, the LUT table will have a lot of "holes" and as such linear interpolation is the best interpolation

method possible without encountering interpolation irregularities. For this reason linear interpolation was selected.

5 | Results

In this chapter the results of the previously presented methodology will be discussed. Firstly load specific DEL trends will be analyzed as a function of the yaw misalignment angle and the derating degree of the upstream turbine while DEL variations will be expressed as the percentage increase compared to the reference case which is the uncontrolled condition when both the yaw angle and the derating degree are equal to zero. Insights for all type of loads will be provided but a particular focus on flapwise DEL is adopted, both for its importance and its regularity. This section aims at providing concrete examples of how the model developed in this thesis, responds to different scenarios and it is useful to comprehend the degree of reliability of this method.
Naturally not all the considered cases will be commented since that would be time consuming and most importantly confusing. Instead, of the initial 875 cases, observations on a selection of interesting cases will be presented in order to give a general idea on how the model works and what the overall trends are.
After that the constraint curves will be finally presented and a sensitivity analysis will be conducted on the tolerance allowed for DEL variations.

5.1. Blade root flapwise moment DEL trends

Before commenting on how the control of the upstream turbine can influence the loads of the downstream one, it is useful to analyze what happens in the uncontrolled condition as a function of both the mean wind speed and the lateral offset of the downstream turbine. This can then serve as a baseline on which to contextualize the DEL variation with respect to the relative position of the wake. The general trend of this aspect can be seen in Figure 5.1 for the range of wind speeds and lateral offset considered in this work. Additionally an ambient condition is included as an overall reference; this is the condition in which the upstream turbine operates that is a wind field with no wake effect whatsoever.

As expected the main influencing factor on DELs is the mean wind speed V_m while the offset contributes to a marginal effect most of the times. Even at 13 m/s when this latter effect is strongest, it contributes to variations in the order of 5% when referred to the least

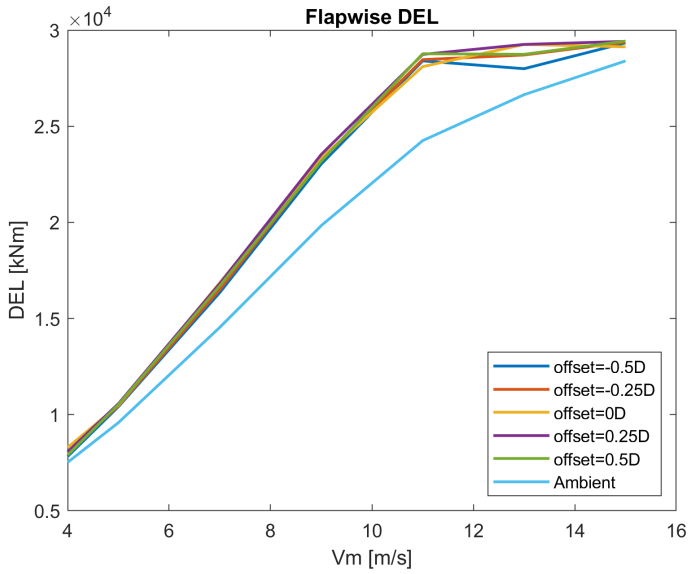

Figure 5.1: Flapwise DEL curve for the uncontrolled case as a function of V_m and lateral offset

loaded case. From the graph the distinction from region 2 and region 3 is also evident since the latter is characterized by a more constant profile as the pitch regulation takes place.
While the influence of the lateral offset is generally limited, it is true that negative offsets seem to obtain lower DEL. As such it was inferred that a wake positioned on the left of the rotor has a negative influence on the flapwise DELs. This is relevant because, as it will be clear, this trend can also be recognized when considering the lateral steering of the wake effect on the DEL variations.
Now that the reference condition has been framed the influence of the upstream control will be discussed.
By how the wake was modelled four main effects can be seen in action:

- the increase in DELs due to the added turbulence in the wake region
- the asymmetrical effects of the wake position relative to the hub as previously described for the reference condition.
- a reduction in the mean wind speed due to the wake deficit which generally causes, when all the other conditions are fixed, a reduction in the DEL
- a steady state fluctuation in mean wind speed perceived by the blades, conceptually similar to the natural shear one, due to their rotation in and out of the wake region. For the cases considered, this effect is rather limited and suppressed by the previous ones mostly because of the actual variations along the rotation which never exceed

the order of 1 m/s

All of the above effects are always present at the same time in the conditions considered and they often interact in unpredictable ways that makes identifying stable trends not always possible.
Nonetheless the greatest influence by far is the increased turbulence intensity in the wake region and it is this factor that usually determines whether the loads increase or decrease.

The upstream control acts on this effects by yawing or derating, in particular:

- yawing: decreases the peak of the gaussian wake deficit and, as such, controls indirectly the width of the region with increased turbulence since, because of the double condition explained in Section 3.4, a lower A implies also a less sharp gaussian; changes the lateral coordinate of the wake center by steering the wake, in particular by how the reference system was defined, positive yaw angles steer the wake to negative values of y
- derating: decreases strongly the peak of the gaussian wake deficit with the same implications reported above and reduces the impact of steering the wake, especially for V_m just below rated wind speed

Both types of control do not have a significant impact on σ which is largely dependent on just V_m.
Some examples will now be presented in order to better understand how the flapwise DEL is influenced by the effects aforementioned.
By considering the condition in which there is no lateral offset the effect of the wake position relative to the hub can be appreciated. For this condition, reported in Figure 5.2, the rotor is always located inside the wake, even when upstream turbine is completely steered to $\pm$ 25°. This is because, as shown in Chapter 4.3, the lateral deviation of the wake center is at best around one fourth of a rotor diameter which is clearly not enough to impact substantially the loads of the downstream turbine.
For this reason the most influencing factor for these conditions is the wind speed dependent DEL for the reference conditions shown in Figure 5.1. In particular, for Vm=4, 7 and 13 m/s the worst lateral offset is exactly 0D and for this reason any change in yaw or derating generally manages to lower the flapwise DEL. Viceversa for Vm=11 m/s the best lateral offset is 0D therefore any control of the wake via the upstream turbine results in increased flapwise DELs.

For these conditions derating tends to increase, even if by a limited amount, the fatigue effects. This is probably due to the fact that by derating the gaussian wake tends to

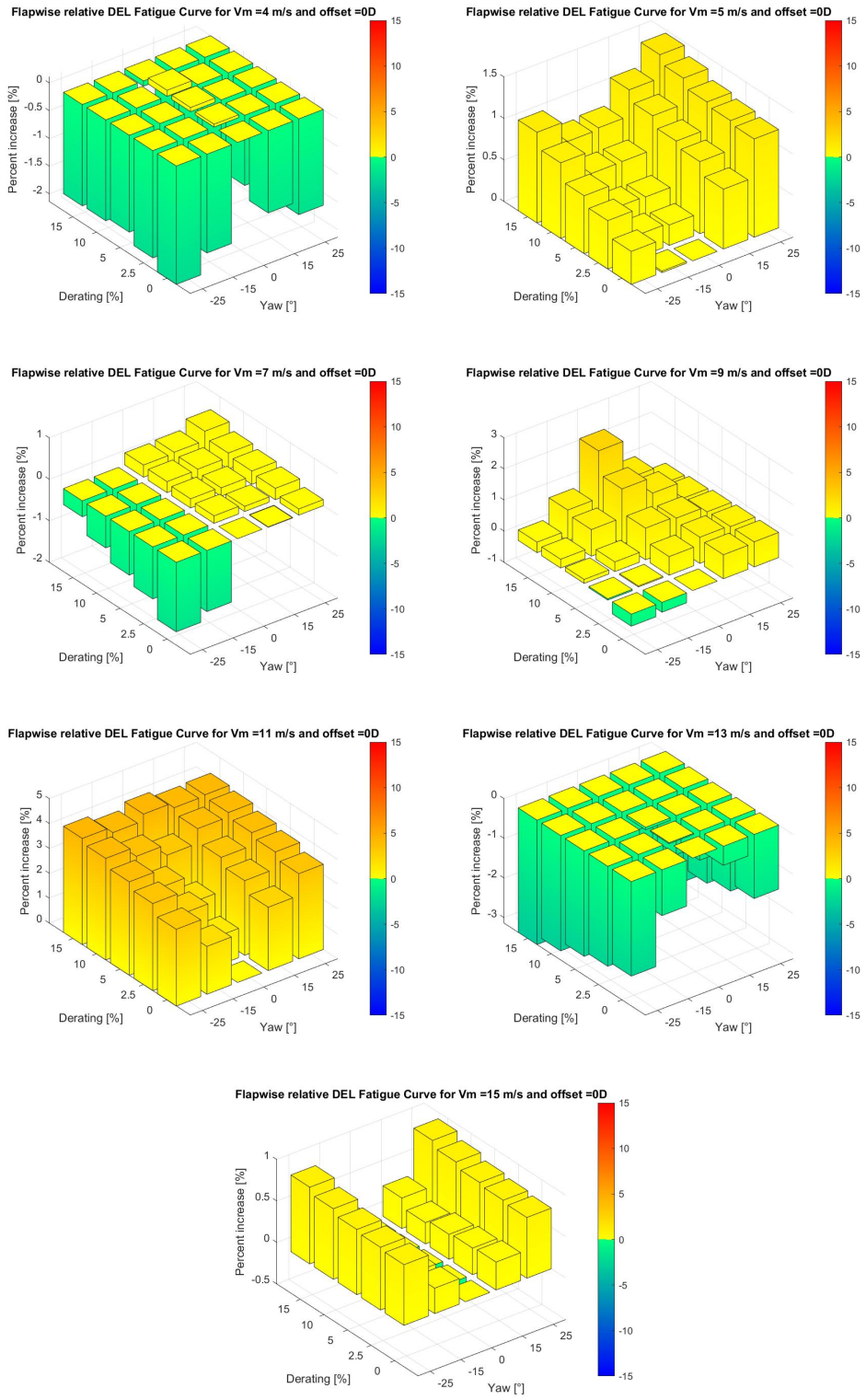

Figure 5.2: Blade root flapwise DEL trends for no lateral offset condition

flatten out, increasing the mean wind speed seen by the downstream turbine and causing

higher loads.

As the lateral offset of the downstream turbine increases to -0.25D some directional effects can be observed. For example, from Figure 5.3 it can be seen that as the yaw increases to -25° the rotor starts to experience the ambient turbulence intensity on its right side but clearly not by a significant amount so the variation in DEL can be explained only by the change in intensity and lateral position of the wake deficit. The exact reason for why this happens is unclear but can only be attributed to the difference in effective mean wind speed due to the wake deficit.
This is also supported by the fact that, at fixed yaw misalignment angle, as the degree of derating increases, DELs tend to increase as well. This correlation may be explained by the fact that derating increases effective mean wind speed adjusted to the wake deficit (Figure 5.4) and as such impacts the fluctuations in aerodynamic loads.

By increasing even more the lateral offset up to 0.5D the effect of steering away the wake, and with it the increased turbulence, can finally be appreciated. Considering the case with V_m=9 m/s and offset=-0.5D in Figure 5.5 a clear asymmetry with respect to the wake lateral position is seen. Negative yaw misalignments allow the wake to be moved away and as such reduce significantly the turbulence intensity experienced by the blades. For conditions where the yaw misalignment is not enough to steer the wake away, similar reasonings to the case with Vm=9 m/s and offset=-0.25D apply.
The model also captures the same trend for the opposite lateral offset 0.5D as in Figure 5.6 where clearly the beneficial yaw direction is switched. The divergence in terms of quantitative variation in DELs may be instead explained by the the baseline difference that exists between lateral offsets as in Figure 5.1. Indeed the reference condition for offset=-0.5D is already the optimal one in terms of layout and as such the possible improvements are limited while for offset=0.5D this is not true.

Lastly it is also worth to note that for all conditions considered in this work the flapwise DEL percent variation remains always limited in the range [-8, 4] %. This indicates that at the very least the impact of upstream control on the downstream turbine DEL estimated with this model is rather modest or, at worst, the deterministic contributions are generally eclipsed by the stochastic contributions and as such more random seeds should be used for the LUT construction process.

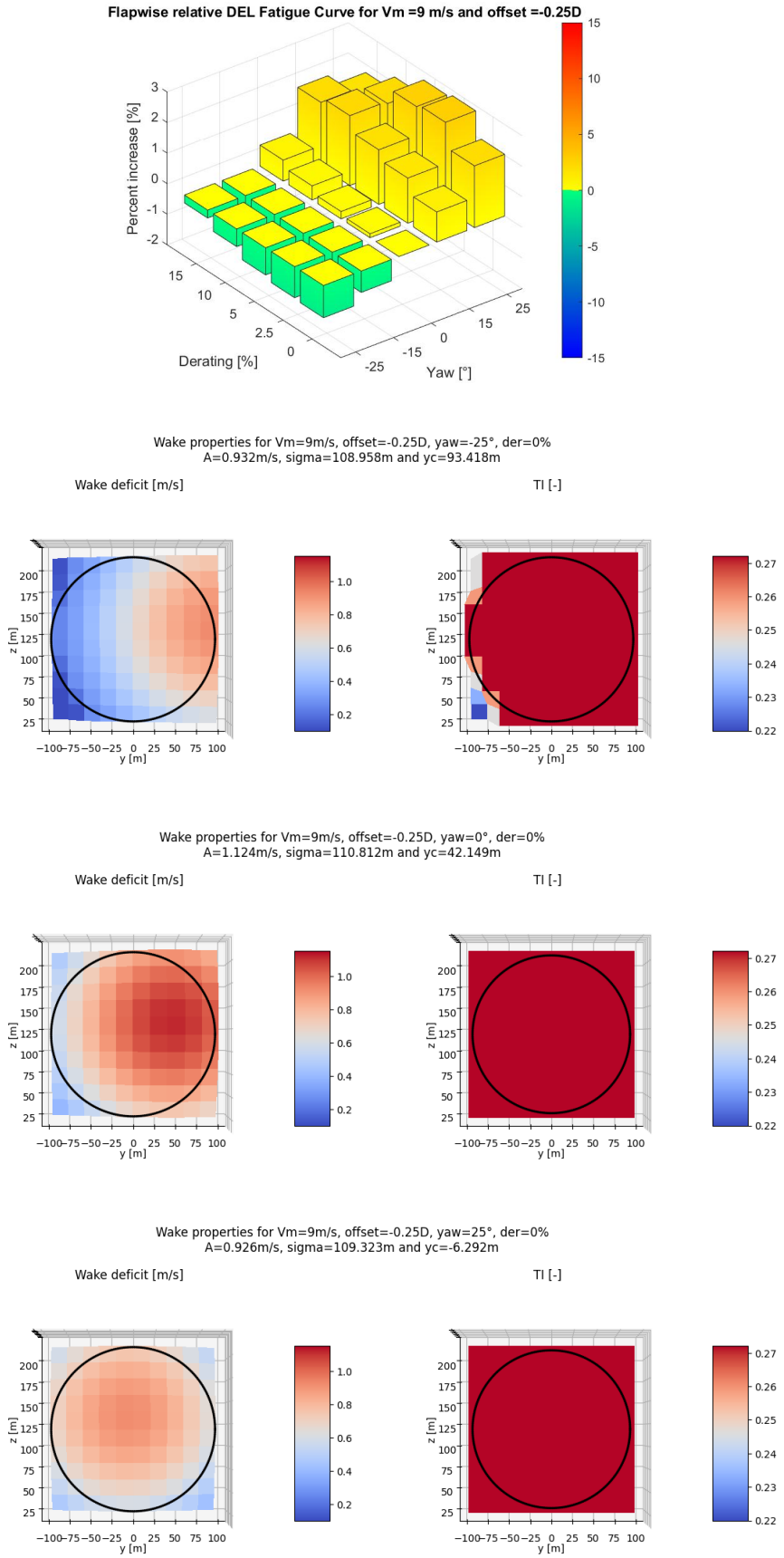

Figure 5.3: Blade root flapwise DEL trends and wake properties at the rotor for V_m=9 m/s and offset=-0.25D at zero derating. The black circle represents the rotor disk.

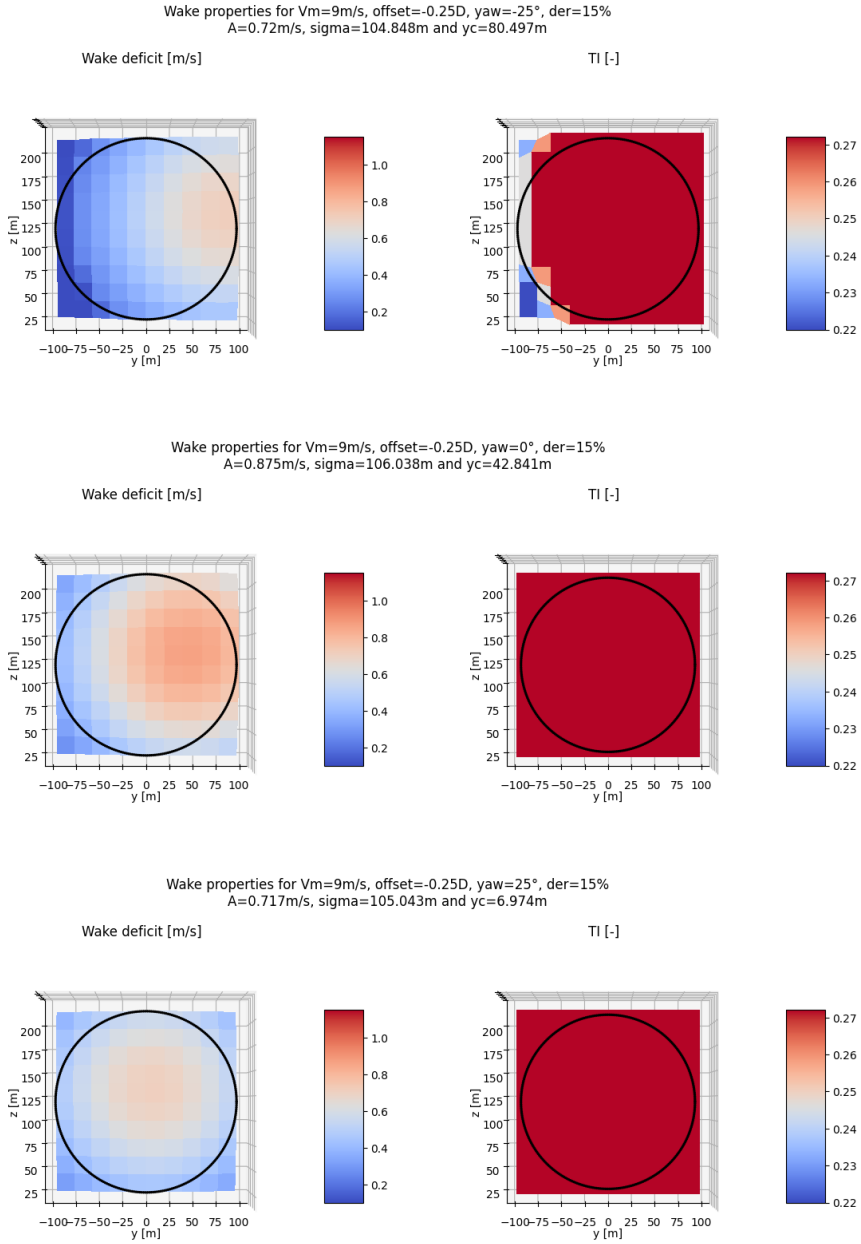

Figure 5.4: Blade root flapwise DEL trends and wake properties at the rotor for V_m=9 m/s and offset=-0.25D at 15% derating. The black circle represents the rotor disk.

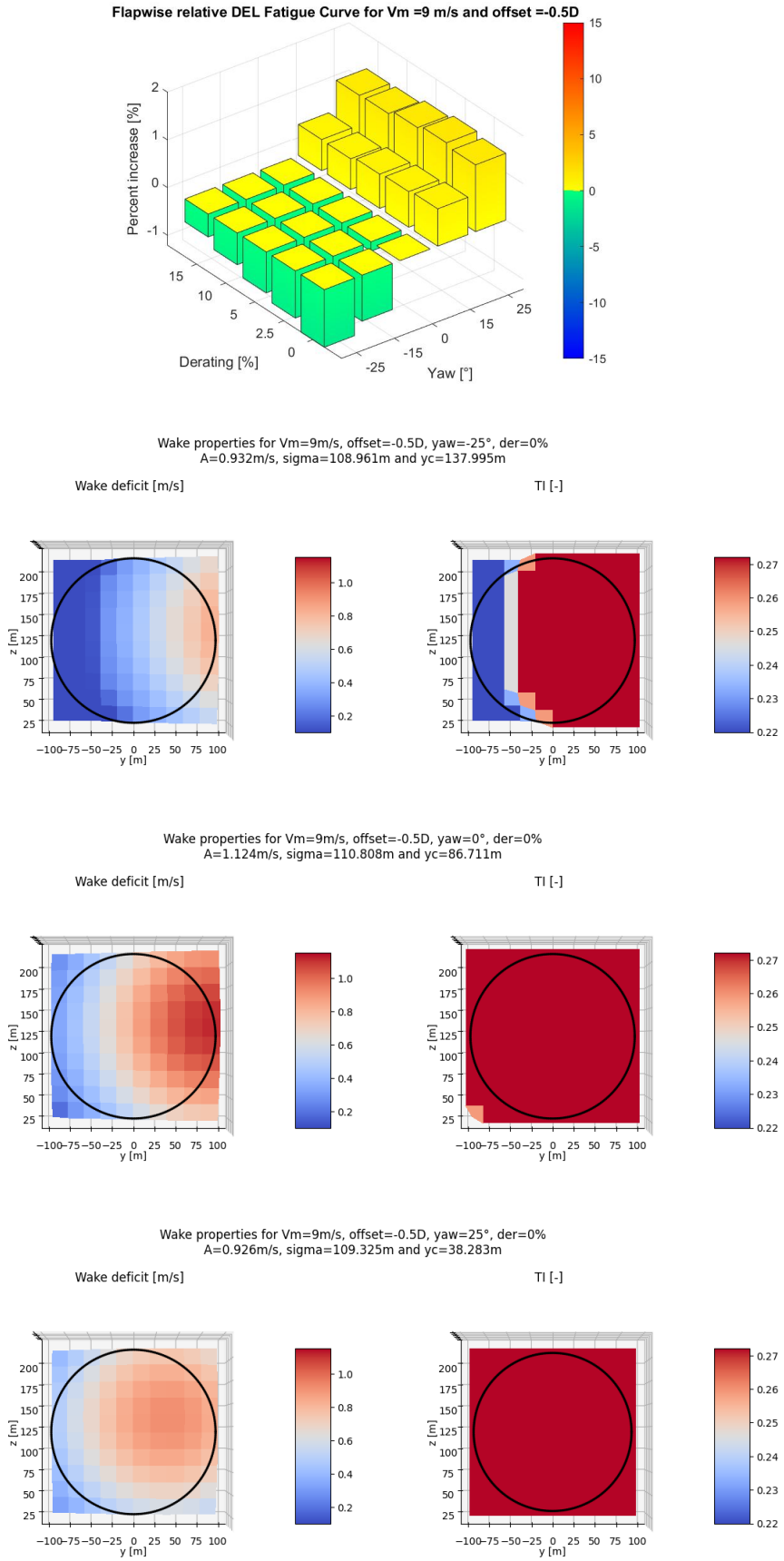

Figure 5.5: Blade root flapwise DEL trends and wake properties at the rotor for V_m=9 m/s and offset=-0.5D at zero derating. The black circle represents the rotor disk.

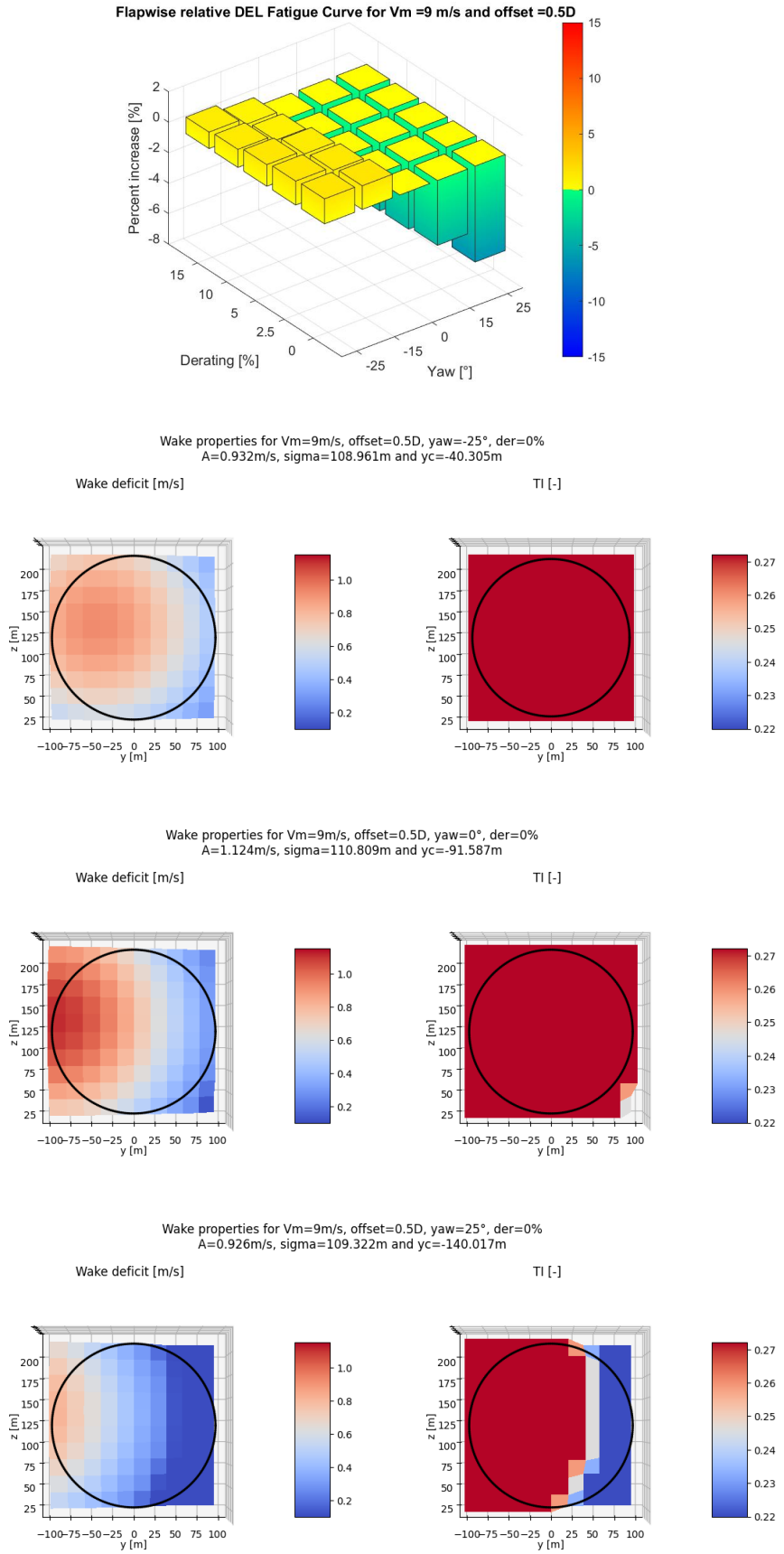

Figure 5.6: Blade root flapwise DEL trends and wake properties at the rotor for V_m=9 m/s and offset=0.5D at zero derating. The black circle represents the rotor disk.

5.2. Blade root edgewise moment DEL trends

The edgewise bending moment is largely dependent on gravity loads therefore the upstream control should not influence this DEL significantly. By observing Figure 5.7 it is clear that this is not true for V_m=11 m/s where just by shifting the downstream turbine laterally the DELs increase by 20% compared to the full wake immersion case.

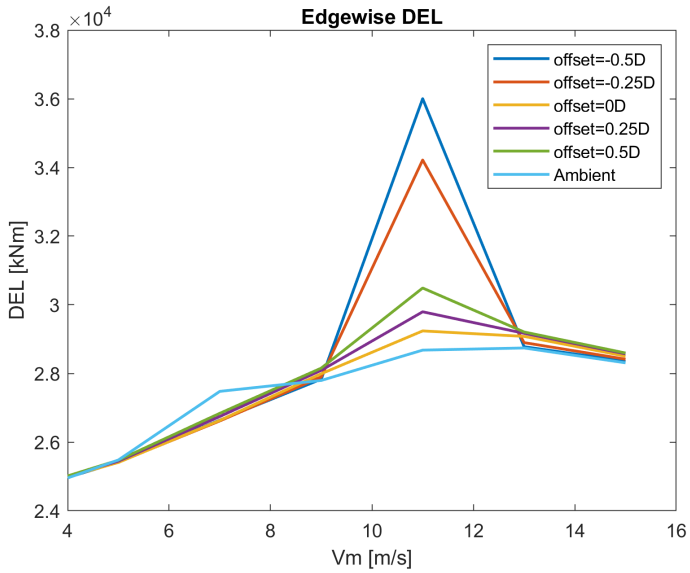

Figure 5.7: Edgewise DEL curve for the uncontrolled case as a function of V_m and lateral offset

To investigate the reason why this happens the time history of the edgewise bending moment was analyzed at V_m=11 m/s for both the reference upstream condition (ambient) and for offset=-0.5D. The main results are reported in Figure 5.8.
The first important information that can be inferred is that the difference in time history of the edgewise bending moment of the two cases lies in the first 200 seconds and more notably in the first 100 seconds during the transient between quasi-steady state of the first 50 seconds and the actual wind inflow representative of the waked case. After this relatively short period of time the two cases show almost no difference at all.
Interestingly because of this initial difference the peak at the first edgewise mode of 0.93 Hz sharply increases by a whole order of magnitude.
By looking at the history of the wind speed at hub height one can realise that the offset condition, due to the higher turbulence, reaches significantly stronger wind speeds in the first few seconds.
This suggests that the problem lies in the control of the wind turbine that, because of the sharp increase in the transition phase after the quasi-steady state, cannot keep up with

the fast changing inflow. Additionally, for V_m=11 m/s, the turbine is also working at the boundary between region 2 and region 3 meaning that a failure in maintaining the control of the desired operating conditions may result in strong variations in the loads.
The fact that this increase in DELs does not occur, at least as sharply, for the offset=0.5D indicates that indeed the lateral position of the wake can have an influence on the edgewise DELs but because of the aforementioned problem, its true impact cannot be deduced from this cases alone. Changing the random seed used for generating the wind time series may be one way to establish if this effect is physical or it is just related to a problem in how the simulations were conducted, in particular to the definition of the initial conditions.

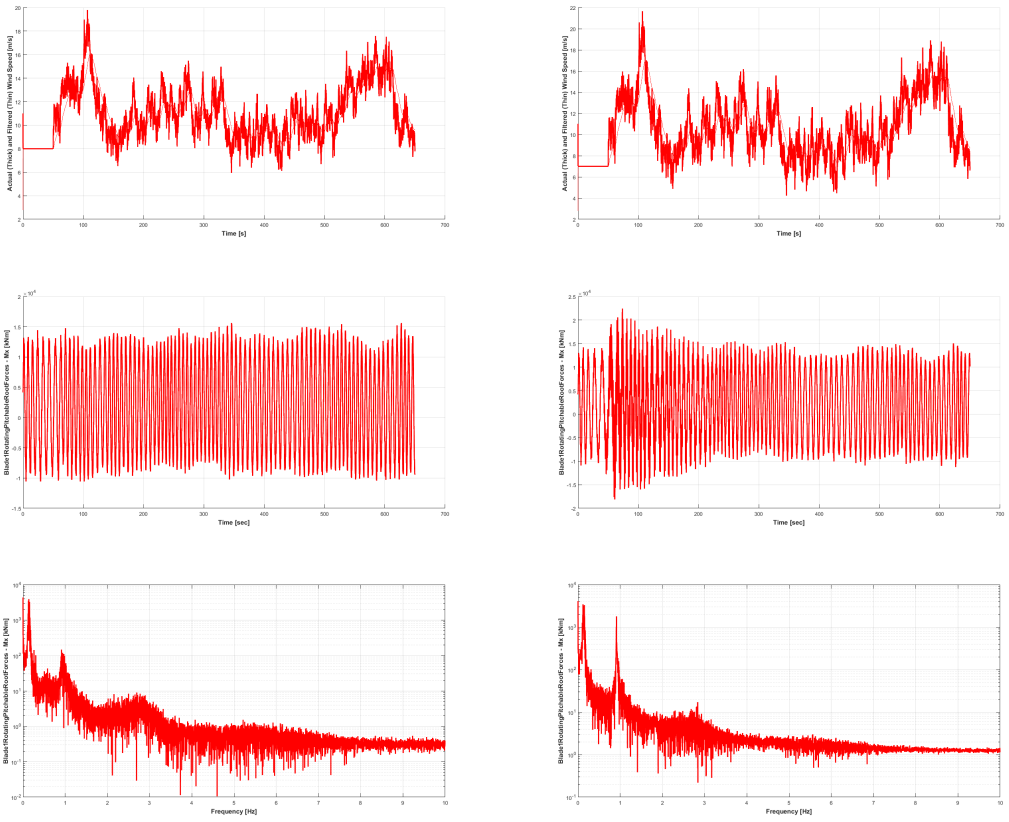

Figure 5.8: Wind speed at hub height, edgewise bending moment and its Fourier transform for ambient condition (left) and offset=-0.5D (right)

For all the other wind speed conditions the edgewise DEL percent variation with respect to the corresponding reference conditions are always limited in the range [-0.4, 0.8] % and are therefore considered not interesting for this work.

5.3. Tower base side-to-side moment DEL trends

Interestingly the SS DELs seem to be most influenced load by the position of the wake deficit and, unlike the blade loads, they peak before rated wind speed, at V_m=9 m/s. As it can be seen from Figure 5.9 DELs vary significantly just from the lateral position of the wake center reaching for V_m=9 m/s a maximum of about 10% when shifting the turbine from 0D to 0.5D. As for the flapwise DELs these curves depict how a change in the lateral

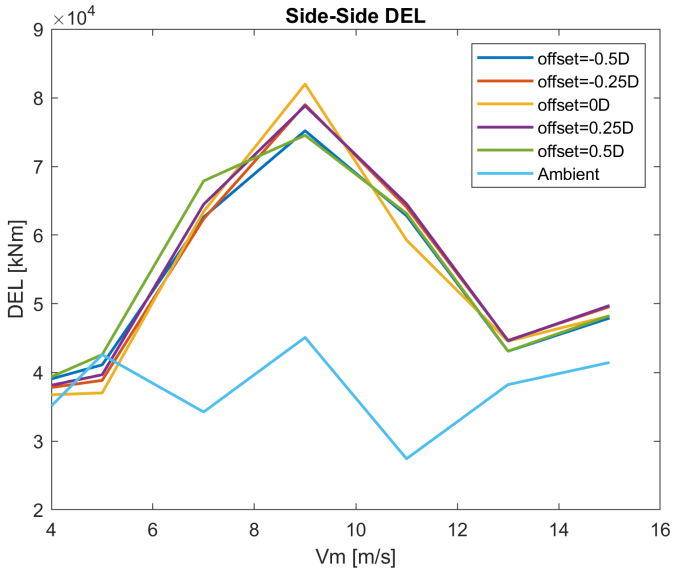

Figure 5.9: Side-to-Side DEL curve for the uncontrolled case as a function of V_m and lateral offset

position of the wake influences the DEL variation with respect to the yaw misalignment angle. In particular for $V_m \geq$7 m/s the trend of lower loads as the wake center is moved away from the rotor, generally holds true but for lower wind speeds (Figure 5.10) the opposite is true. This may be due to the fact that at such low V_m the downstream turbine always operate in the increased turbulence region and as such DELs vary mostly due to the wake deficit position. Since, for these conditions, a centered wake deficit is preferable, yaw angles that move the wake closer to the rotor center actually reduce DELs.
Even when considering the impact of upstream control on DELs the variations are much more notable and stay in the [-30, 40] % range. An example of this can be found in Figure 5.11.
For these conditions, a wake that is steered away from the rotor induces great percent reductions in SS DEL and viceversa, hinting once again at a strong correlation with the wake lateral position.

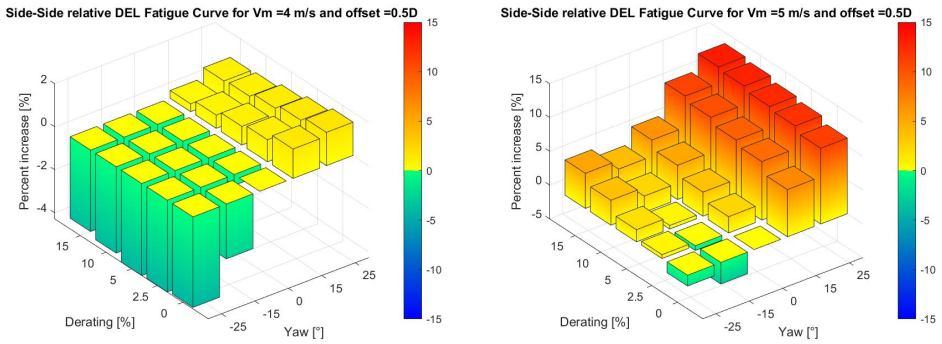

Figure 5.10: Tower base side-to-side DEL trends for V_m=4,5 m/s and offset=0.5D.

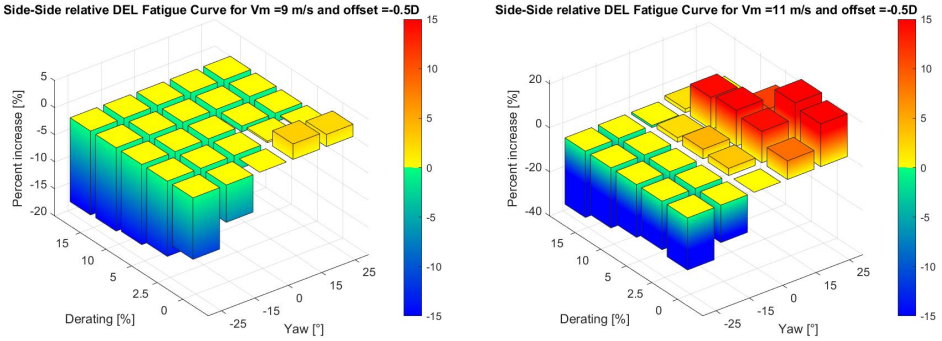

Figure 5.11: Tower base side-to-side DEL trends for V_m=9,11 m/s and offset=-0.5D.

5.4. Tower base fore-aft moment DEL trends

Lastly, considering the tower base FA DELs, they appear more aligned with the blade loads from the point of view of the lateral offset's impact on the shape of the curve (Figure 5.12), since, at least below its peak at V_m=9 m/s, DELs do not vary as much as the SS ones just from a lateral shift of the wake.

Furthermore the upstream control's effect on the DELs variations is much more limited, always in the [-6, 6] % range, with the only significant negative impact at V_m=11 m/s when the OD offset condition is the least loaded one. For all other wind speeds it is almost always possible to reduce or equal the reference DELs as long as an appropiate choice of yaw angle - derating degree is chosen. The exceptions being V_m=4,5 m/s for which DELs increase but not above around 1.5% which may very well be within the margin of error of this method. In Figure 5.13 some interesting cases are reported to show how steering the wake away from the rotor is useful also for the FA DELs.

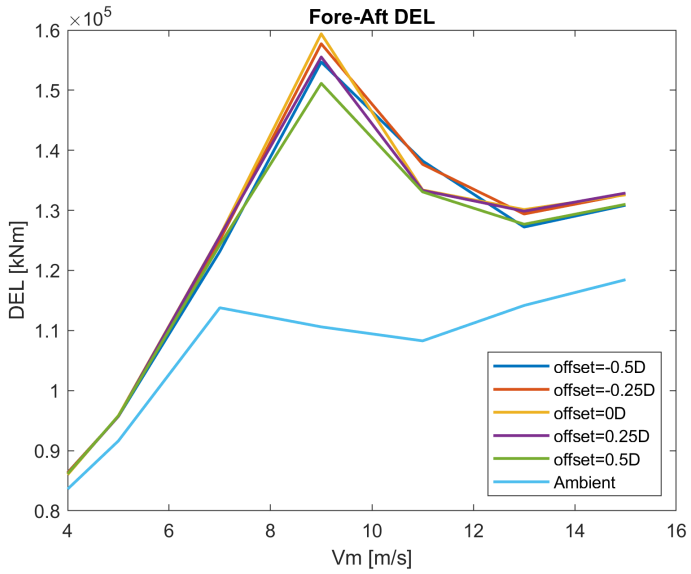

Figure 5.12: Fore-Aft DEL curve for the uncontrolled case as a function of V_m and lateral offset

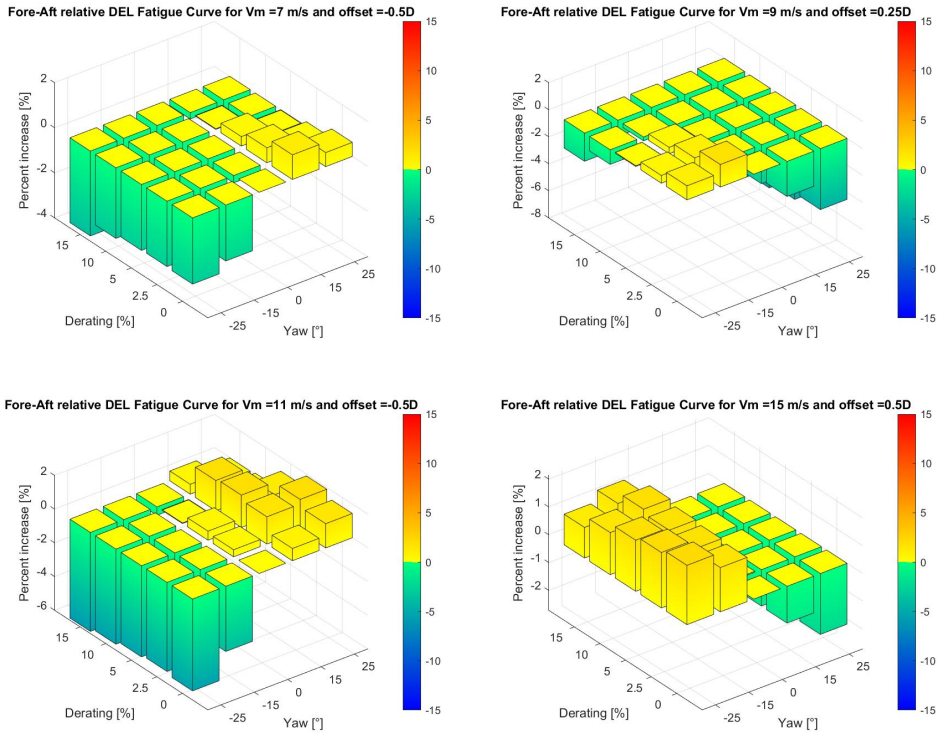

Figure 5.13: Tower base Fore-Aft DEL trends for a compilation of cases

5.5. Constraint curves

The constraint curves that will be presented in this section are the final results of this thesis. They provide information on which yaw misalignment angle-derating degree set-points are acceptable from a fatigue load point of view and they are a function of only the direction of the wind (lateral offset) in such a way that would enable wind farms to be easily and safely controlled independently of the chosen optimization criterion.
Even though in this work it was not possible to evaluate the implications of these curves in a comprehensive framework of constrained optimization, they still remain useful to verify general trends and consider possible improvements of the method.
In order to construct the constraint curves, for each lateral offset all four DELs are evaluated for every wind speed and yaw misalignment angle-derating degree combination for the domain considered. Subsequently each yaw-derating combination is considered acceptable for a specific lateral offset, if the four DELs are lower than the ones of the respective uncontrolled condition for each wind speed considered.
The reasoning behind the choice of the reference case is that it allows to understand how to improve the downstream turbine fatigue life from the loads that it will inevitably experience rather than how to control the upstream turbine such that the downstream one operates in design conditions. Additionally, the method developed in this work seems to indicate, from the DEL curves previously presented, that the downstream turbine will always experience DELs much more intense than the upstream condition and, as such, in this sense no yaw-derating combination would be acceptable.

5.5.1. Overall constraint curves

In this section constraint curves built on all DELs and every wind speed will be presented. From the results of the previous section it is to be expected that no actual condition is able to satisfy the conditions to be acceptable and, as a matter of fact, it is exactly like that. This is because of the different trends that each of the four loads has, combined with the fact that every increase in DEL, no matter how small, automatically excludes that yaw-derating combination for every wind speed at a specific offset. A clear example of this are the edgewise DELs that even though are limited in the [-0.4, 0.8] % range for $V_m \neq$11 m/s, they may compromise a large amount of, otherwise acceptable cases.
In order to both relax slightly this constraint and account for some margin of uncertainty for this proposed method, the constraint curves were calculated again but with a tolerance of 5% when comparing to the reference case. These curves are represented in Figure 5.14.

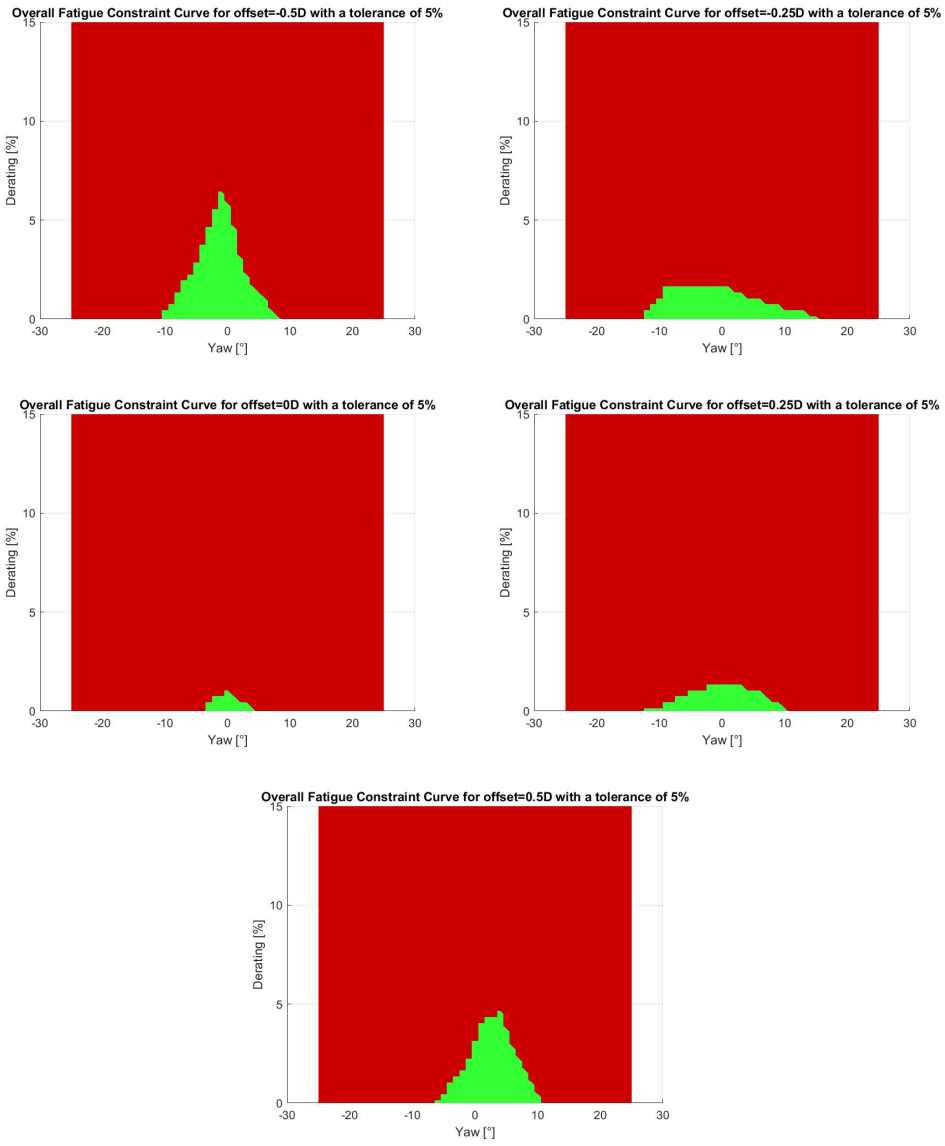

Figure 5.14: Constraint curves for different lateral offsets with a tolerance of 5%

The constraint curves are still mostly composed of not acceptable cases but at least some effects can be appreciated.
One of which is certainly the negative effect that derating seems to have on downstream DELs. This is most likely due to the fact that its influence on the added turbulence was not implemented in this model. As such it only contributes to having a higher V_m over the rotor disk which generally increase DELs.
Furthermore as the lateral offset increases in modulus, this effect seems to be mitigated and higher derating degrees can be achieved as well as a potentially greater area of upstream control, with a slight preference for yaw angles that steer the wake away from the rotor.

5.5.2. Constraint curves excluding side-to-side DEL

Due to the fact that for the tower base the FA DEL is the design load, another set of constraint curves was generated to investigate how excluding the SS DELs affects the allowable control area.
Again if the tolerance is kept at 0% no combination of yaw-derating is acceptable but by increasing it to 2% and 5% the results change significantly.

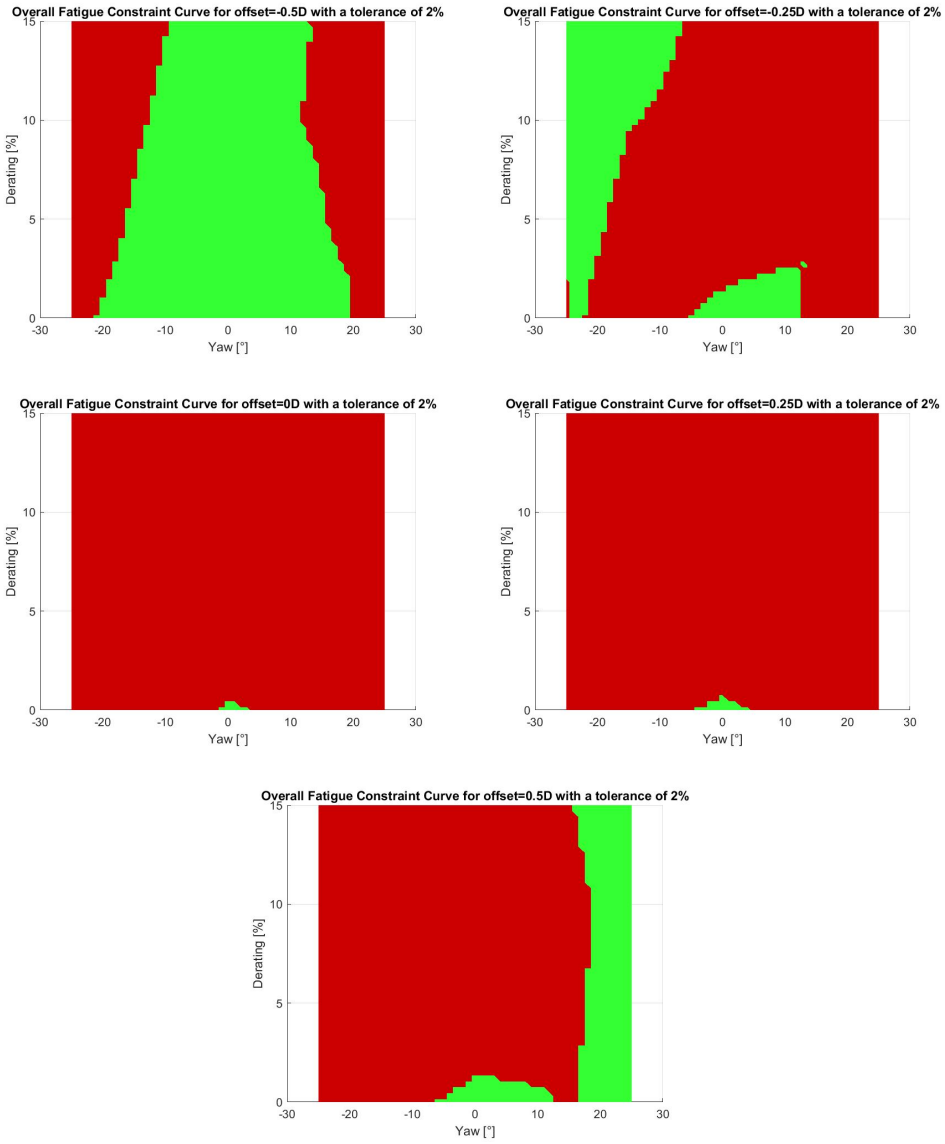

Figure 5.15: Constraint curves excluding SS DELs for different lateral offsets with a tolerance of 2%

As it can be seen from Figure 5.15 and 5.16 the impact of SS DELs was indeed significant and, while for lateral offset of 0D and 0.25D other loads still constrain the area of control,

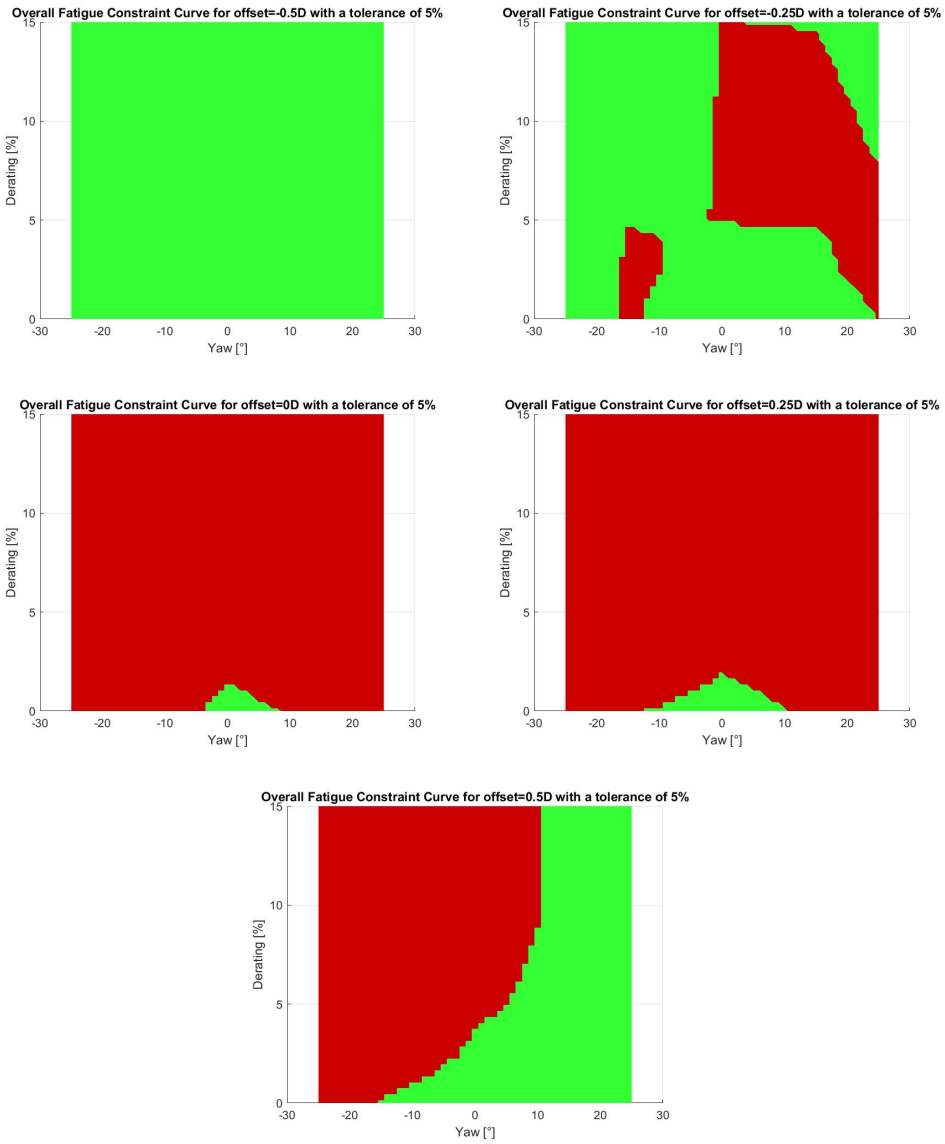

Figure 5.16: Constraint curves excluding SS DELs for different lateral offsets with a tolerance of 5%

for other offsets the possibilities of upstream control grow.
Another interesting aspect that arises from these graphs is a strong asymmetry over the lateral offset, in particular negative offsets seem to be much more preferred. This is easily explained by the unexplained edgewise DELs trend at V_m=11 m/s (Figure 5.17). When comparing the two sets of curves is evident that the regions of the constraint curve that are missing are mirrored by abnormally large edgewise DEL variations.
It is then obvious that what is happening at V_m=11 m/s along the edgewise direction is what is stopping the control to have more freedom for offsets=0D, 0.25D and 0.5D. To test this another set of constraint curves was built that also excludes V_m=11 m/s and, as

expected, every yaw-derating combination is then acceptable (Figure 5.18).

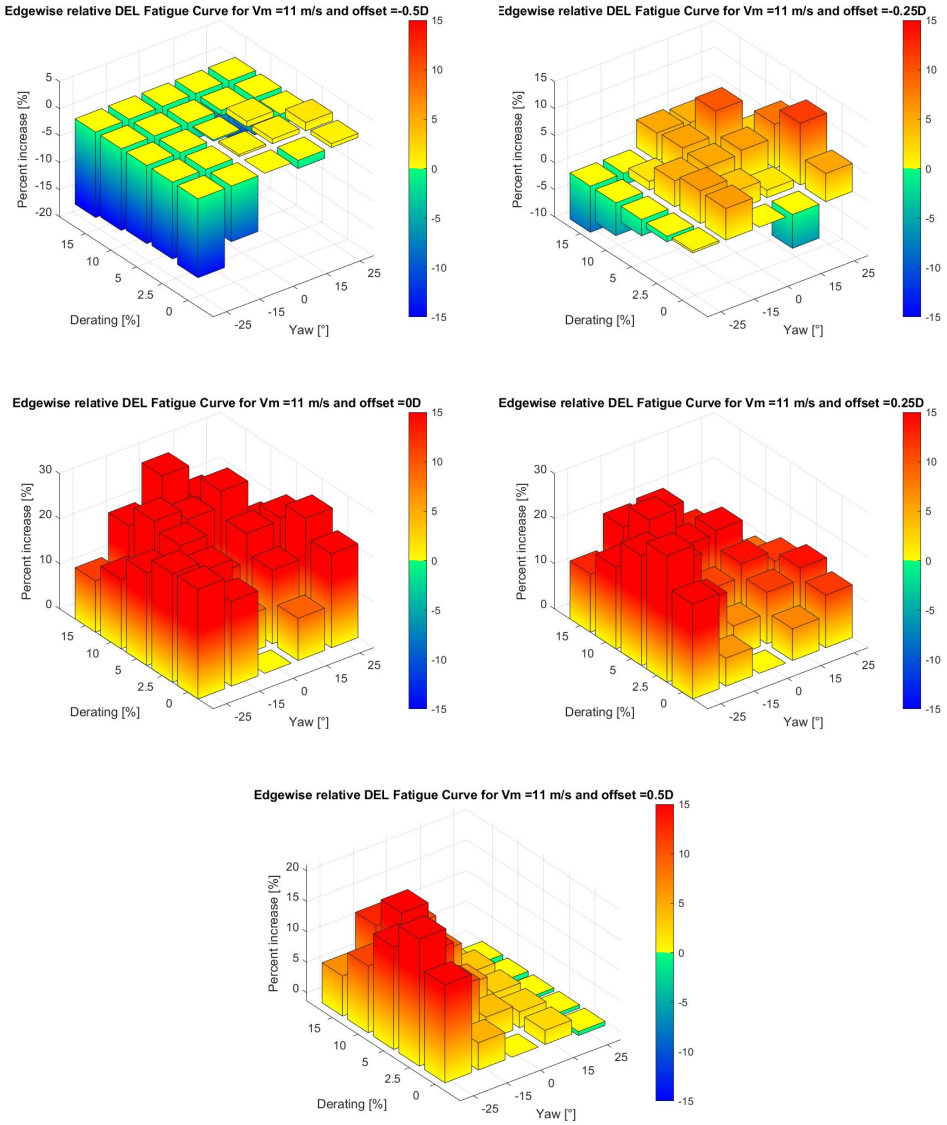

Figure 5.17: Blade root edgewise DEL trends for V_m=11 m/s

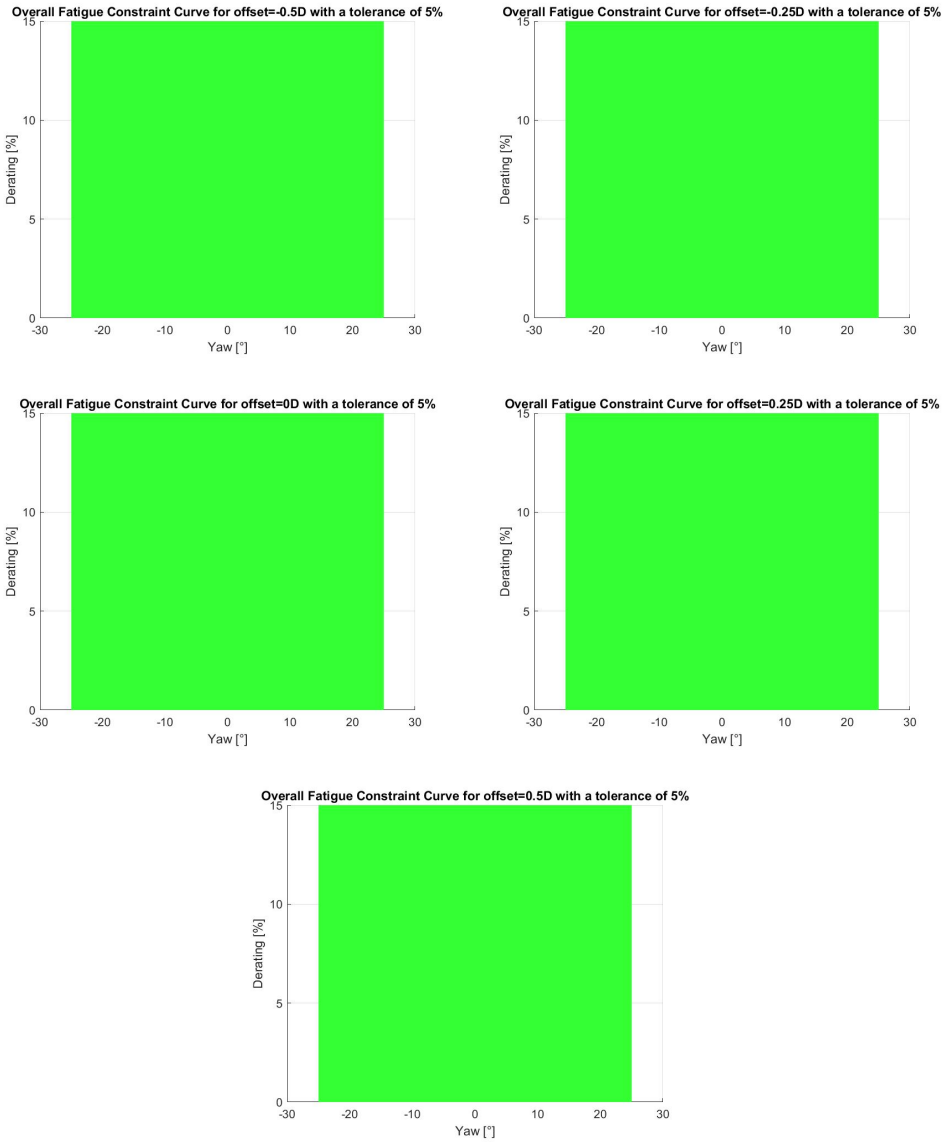

Figure 5.18: Constraint curves excluding SS DELs and V_m=11 m/s for different lateral offsets with a tolerance of 5%

6 | Conclusions and future developments

The purpose of this thesis was to investigate how the control of the wake through axial induction reduction and yaw-based wake steering of the upstream turbine may influence the fatigue loads of the downstream one.
To achieve this goal, first the wake properties for different environmental and operational cases were studied through the use of a wind farm engineering model applied to a state-of-the-art wind turbine model. From there, in a framework that aims at reducing as much as reasonably possible the computational time, a set of significant cases were selected on the basis of their steady state wake properties. Through the two regions wake model developed, these wake properties are used to generate wind time series as input for the aeroelastic software Cp-Lambda. The fatigue loads look up table was then successfully created from the output of these simulations. The main conclusions of this work can be briefly summarized in the list that follows:

- With the conceived method it is possible to estimate the DELs of a downstream turbine as long as the wake that impinges on it can be described with a gaussian shape.
- The wake model developed can capture the effects related to different operating conditions between inside and outside of the wake. Furthermore the asymmetry of the problem with respect to different wind directions can be observed as well.
- With the current model derating the upstream turbine usually results in a worsening of the condition of the downstream one since the decrease in turbulence intensity in the wake is not accounted for.
- The main factor affecting the downstream DELs is by far the area of added turbulence intensity. Nevertheless whenever the downstream rotor is always inside the added turbulence intensity region, no matter the yaw angle of the upstream turbine, the position of the wake deficit relative to the hub seems to have a considerable effect as well.

- Flapwise DELs variations with respect to the reference uncontrolled condition, are always in the range [-8, 4] % indicating some potential for AWC.
- Edgewise DELs variations with respect to the reference uncontrolled condition, are as expected negligible. For V_m=11 m/s there is evidence that the wake position may influence significantly these variations but it may as well be an effect specific to the seed and to the initial conditions chosen.
- Side-to-side DELs have by far the strongest dependence with respect to both the added turbulence intensity region and the position of the wake. Its variations are in the range [-30,40] % and can reach up to double the value obtained with an unwaked turbine.
- Fore-Aft DELs variations with respect to the reference uncontrolled condition, are always in the range [-6, 6] % and generally follow the same trends as the flapwise DELs.
- The constraint curves generated on the basis of the four DEL variations point to the non-existence of yaw-derating combinations that may reduce all four DELs and for every wind speed due to the different trends of each one of the loads.
- If some tolerance is included in the generation of the constraint curves to emulate a reasonable uncertainty of the model and if the outlier cases at V_m=11 m/s are excluded, significant more freedom is allowed to the upstream wind turbine control.

The main problem of the model is that it may be excessively conservative in both the actual correlation used for the added turbulence intensity and in the extension of the region that is subject to the wake turbulence. This is also reflected by the fact that the model suggests that even uncontrolled conditions experience DELs that are significantly higher compared to the unwaked condition. While this could be possible, its extent is quite certainly exaggerated, otherwise the current state of wind farms that are more than a decade old, would be much worse. Additionally, as mentioned earlier, the decision taken out of simplicity, to neglect the dependence of the added turbulence intensity from the derating degree of the upstream turbine plays an important role in this regard too.

For the reasons mentioned, certainly the most interesting next step for research would be to improve the fidelity of the model by:

1. choosing a more refined correlation for added turbulence intensity
2. splitting the inflow in more than two regions, possibly four overall regions with three of them being necessary to more accurately describe the profile of the added

turbulence intensity

3. including the effects of wake meandering

Furthermore, the increased in turbulence in the wake paradoxically causes, if the wake deficit is not strong enough, the wind speed to be sometimes higher in the wake compared to the ambient condition. This is clearly not physical and should be corrected.
Moreover by utilizing just one seed for the generation of the time series, the results could very well be contaminated by stochastic effects drowning out the real trends of the control. Therefore an increase in the number of seeds could be certainly useful to test the approach, even if the computational burden would certainly increase.
Another possible development would be to consider the effect of changing the wind turbines of the wind farm, to see if the same trends observed in this work occur.
Lastly, from an AWC point of view, it would be surely interesting to know how much an hypotetical steering of the downstream turbine would influence the DELs.

Bibliography

[1] Federico Isella. Combining yaw redirection and static axial induction in a ultimate-load-constrained wind farm control. Master's thesis, Politecnico di Milano, Piazza Leonardo Milano, 12 2022.

[2] IRENA. Wind energy statistics, 2022. URL `https://www.irena.org/Energy-Transition/Technology/Wind-energy`.

[3] Eiman Tamah Al-Shammari et al. Comparative study of clustering methods for wake effect analysis in wind farm. 2016.

[4] T Ashuri et al. Integrated layout and support structure optimization for offshore wind farm design. 2016.

[5] Tony Burton et al. *Wind energy handbook*. 2011.

[6] Gianluca Dadda. Impact of combinations of wind farm controllers on wind turbine loads. Master's thesis, Politecnico di Milano, Piazza Leonardo Milano, 04 2021.

[7] Ervin Bossanyi. Combining induction control and wake steering for wind farm energy and fatigue loads optimisation. 2018.

[8] Mendez Reyes et al. Validation of a lookup-table approach to modeling turbine fatigue loads in wind farms under active wake control. 2019.

[9] Ervin Bossanyi. Surrogate model for fast simulation of turbine loads in wind farms. 2022.

[10] NREL. Floris, 2018.

[11] Carlo L. Bottasso et al. Aero-servo-elastic modeling and control of wind turbines using finite-element multibody procedures. 2006.

[12] D.C. Quarton and J.F. Ainslie. Turbulence in wind turbine wakes. 1990.

[13] Rogers A.L. Manwell J.F., Mcgowan J.G. *Wind energy explained: theory, design and application*. 2009.

[14] Robert Braunbehrens and Antonio Segalini. A statistical model for wake meandering behind wind turbines. 2019.

[15] Paul Fleming et al. Initial results from a field campaign of wake steering applied at a commercial wind farm: Part 1. 2019.

[16] Christian Bak et al. Description of the dtu 10 mw reference wind turbine. 2013.

[17] Luca Sartori. *System design of lightweight wind turbine rotors*. PhD thesis, Politecnico di Milano, 2019.

[18] NREL. Turbsim v2.00, 2016.

[19] J. Schreiber et al. Verification and calibration of a reduced order wind farm model by wind tunnel experiments. 2017.

[20] L.J. Vermeer et al. Wind turbine wake aerodynamics. 2003.

[21] Linlin Tian et al. A new three-dimensional analytical model for wind turbine wake turbulence intensity predictions. 2022.

[22] Takeshi Ishihara et al. A new gaussian-based analytical wake model for wind turbines considering ambient turbulence intensities and thrust coefficient effects. 2018.

[23] P.E.J. Vermeulen. An experimental analysis of wind turbine wakes. 1980.

A | Appendix A

This chapter is meant to contain figures that could be interesting but that would have otherwise interrupted the flow of the results chapter too much.

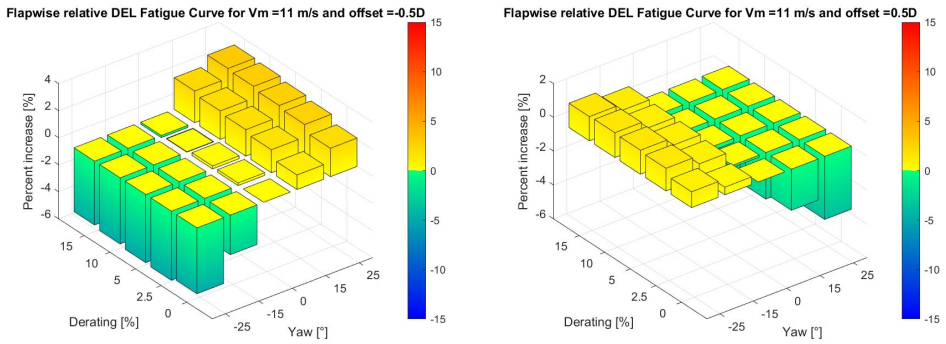

Figure A.1: Blade root flapwise DEL trends and wake properties at the rotor for V_m=11 m/s and offset=±0.5D

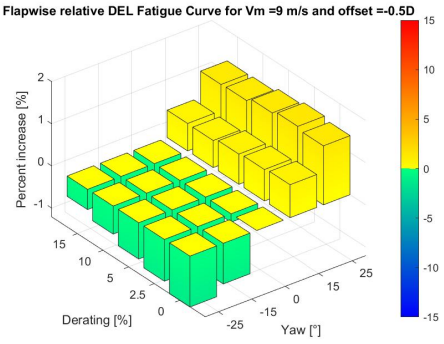

Figure A.2: Blade root flapwise DEL trends for V_m=9 m/s and offset=-0.5D

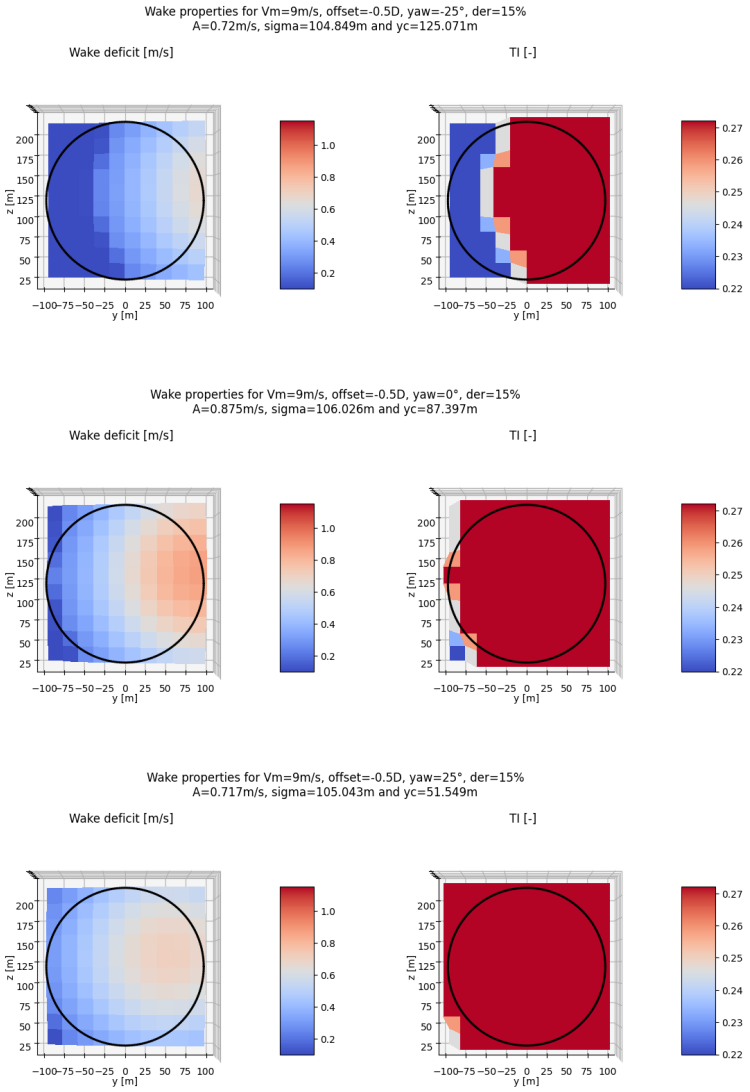

Figure A.3: Blade root flapwise DEL trends and wake properties at the rotor for V_m=9 m/s and offset=-0.5D at derating=15%. The black circle represents the rotor disk.

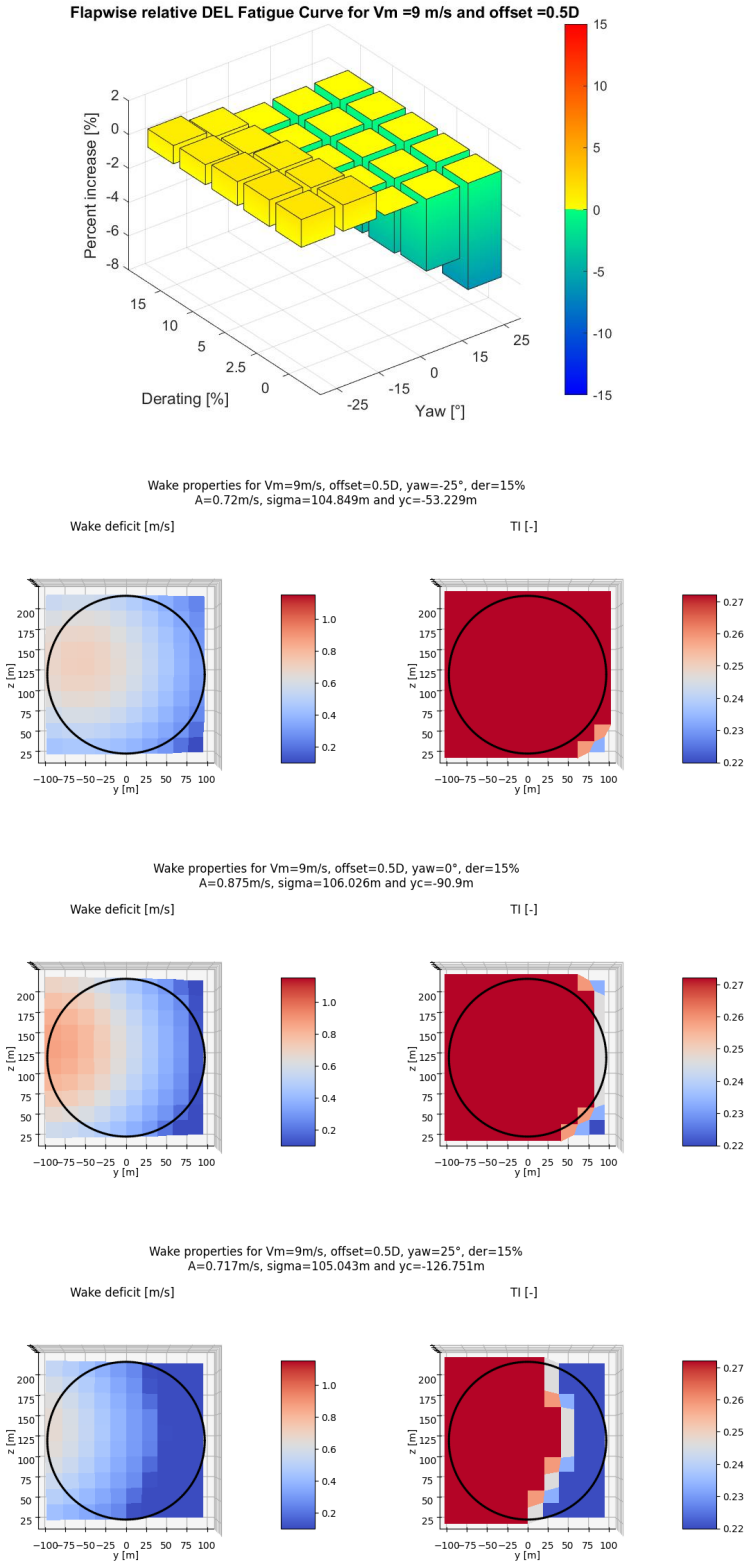

Figure A.4: Blade root flapwise DEL trends and wake properties at the rotor for V_m=9 m/s and offset=0.5D at derating=15%. The black circle represents the rotor disk.

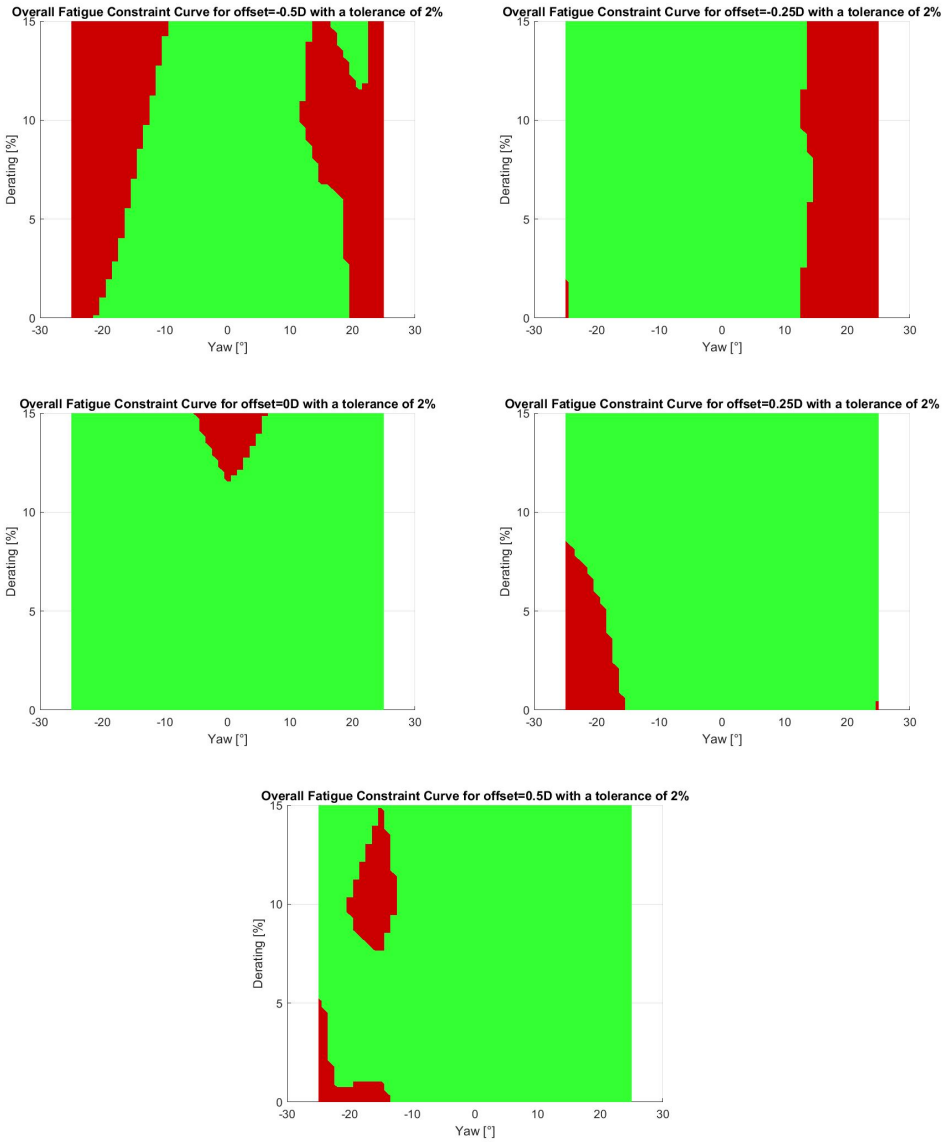

Figure A.5: Constraint curves excluding SS DELs and V_m=11 m/s for different lateral offsets with a tolerance of 2%

List of Figures

List of Tables

List of Symbols

Variable	Description	SI unit
a	Axial induction factor	-
A	Peak of the gaussian wake deficit	m/s
C_T	Thrust coefficient	-
DEL	Damage Equivalent Load	kNm
δ	Gaussian wake deficit	m/s
F	Prandtl's tip loss correction	-
I_0	Ambient turbulence intensity	-
I_{add}	Added turbulence intensity	-
I_w	Wake turbulence intensity	-
λ	Tip speed ratio	-
m	Slope coefficient of SN curve	-
σ	Standard deviation of the gaussian wake	m
V_m	Hub height wind speed	m/s
x	Downstream distance	m
x_N	Near wake length	m
y_c	Lateral coordinate of wake center	m
z_c	Vertical coordinate of wake center	m

Ringraziamenti

Vorrei infine esprimere la mia gratitutine verso coloro che hanno reso possibile questo traguardo.
Innanzitutto, ringrazio i professori Alessandro Croce e Stefano Cacciola per avermi affidato questo progetto e per avermi guidato, tramite prezioni consigli, lungo il suo sviluppo.
Ringrazio i miei genitori, Elena e Luigi, per avermi completamente supportato durante l'intero percorso di studi, senza mai farmi pesare nulla ogni qualvolta fosse possibile.
Ringrazio i miei fratelli, Davide e Pietro, per il supporto emotivo dimostrato durante la scrittura della tesi, nonostante la mia scorbutaggine. In particolar modo ringrazio Davide che, nella sua ostinazione, è da sempre un esempio per me.
Ringrazio i nonni, Iride e Mario, che mi chiamano ingegnere da ben prima della mia iscrizione all'università. Senza il loro duro lavoro non penso che sarei arrivato qui con la stessa facilità.
Ringrazio gli amici di sempre, Corrado, Edoardo, Leonardo, Letizia, Silvia e Simone, per aver migliorato la vita quotidiana e per farmi dimenticare le mie preoccupazioni ogni volta che mi trovo con loro.
E infine ringrazio i compagni di corso tutti, in particolar modo Andrea e Giorgio, per aver reso questi anni passati insieme decisamente più sopportabili.